AD-A052 636 OKLAHOMA UNIV NORMAN DEPT OF ENGINEERING PHYSICS F/G 4/2
A STUDY OF THE APPLICABILITY OF LASERS TO THE MEASUREMENT OF TO--ETC(U)
1976 D A ROSS

UNCLASSIFIED NL

1 OF 2
AD
AD52636

[Dept of Env Physics]
THE UNIVERSITY OF OKLAHOMA
GRADUATE COLLEGE

(1)

(6)

A STUDY OF THE APPLICABILITY OF LASERS TO THE MEASUREMENT OF TORNADO WIND SPEEDS.

(9) Master's thesis,

A THESIS

SUBMITTED TO THE GRADUATE FACULTY

in partial filfillment of the requirements for the

degree of

MASTER OF SCIENCE

(12) 189 p.

(11) 1976

(10) By
DAVID ARNOLD ROSS
Norman, Oklahoma

1976

A STUDY OF THE APPLICABILITY OF LASERS TO THE MEASUREMENT

OF TORNADO WIND SPEEDS

A THESIS

APPROVED FOR THE DEPARTMENT OF ENGINEERING PHYSICS

By

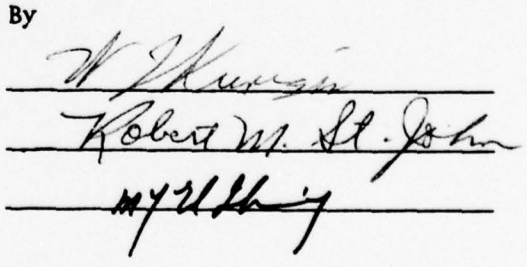

ACKNOWLEDGEMENTS

I would like first of all to thank Dr. William Kuriger for his suggestion of this topic, his encouragement and his thought provoking discussions on the work presented here.

I would also like to thank those people who helped in various ways: Drs. Robert St. John and M. Y. El-Ibiary, who served on my committee; Dr. John McCarthy and Robert Davies-Jones for their illuminating discussions on the phenomena of tornadoes; Dr. Jay Fein for his encouragement and helpful discussions on meteorology in general; and, Mary Lou Stokes who typed the final copy.

Most of all, I would like to thank my wife, Linda, who has endured these last two years with little complaint, much understanding, and lots of love. To her, this work is dedicated.

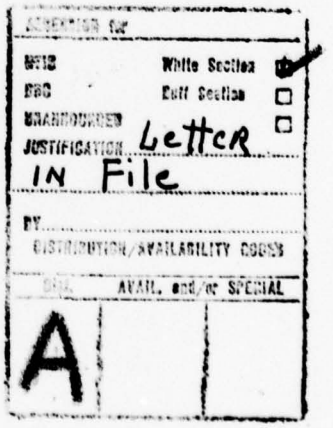

TABLE OF CONTENTS

LIST OF TABLES

LIST OF TABLES (Cont'd.)

LIST OF ILLUSTRATIONS

CHAPTER I

INTRODUCTION

The purpose of this research is to examine the theoretical possibility of using pulsed lasers to determine the velocity structure of the turbulence associated with tornadoes, particularly, the funnel cloud. → cont p 66

The basic structure of a tornado consists of a cloud base, a funnel, and a debris cloud. The cloud base may be visualized as the top of the tornado, connecting the clouds to the tornado funnel. The funnel extends from this cloud base towards the ground; if it does not contact the ground it is usually referred to as a funnel cloud. If the funnel does come in contact with the ground, the severe nature of its turbulence creates a debris cloud which may extend back into the air for several hundred feet. Physically, the tornado may extend from a narrow funnel, with a diameter of several meters, to much larger funnels whose damage paths indicate diameters of over a kilometer. Internal velocities of particles and debris are of the order of 50-80 m/sec, but may exceed 100 m/sec (220 miles/hour).[1] Estimates of tornado velocities and similar turbulence have

---

[1]Robert Davies-Jones and Edwin Kessler. "Tornadoes," *Weather and Climate Modification*, ed., Wilmot N. Hess (New York: John Wiley and Sons, Inc., 1974), p. 553.

come from direct measurements supplied by one of the following methods: doppler radar, doppler lidar*, aircraft probe, and photogrammetry. Each of these techniques is limited by different factors: The radar is limited by a range resolution of about 150 m. The cw-lidar used by Schwiesow, *et al.*, is limited in range to about a kilometer due to power and mobility requirements.[2] Aircraft probe is considered too dangerous for tornadoes and photogrammetry is limited dimensionally.

Of the four techniques, the lidar appears the most promising. However, the range limitation remains a serious problem which can be alleviated by using a pulsed laser; a pulsed laser has the capability to provide considerably more power than a continuous wave laser (cw-lidar) and should thus provide more range.

Proposed Scheme

The proposed scheme consists of analyzing the extinction and backscatter properties of mathematical models of a tornado (based on probable composition) at various wavelengths ranging from 0.5 μm to 10.6 μm. The purposes of the analysis are 1) to determine the power required to project a beam of pulsed laser light through the intervening atmosphere to the tornado, scatter from the

---

[2]Robert F. Abbey, Jr., *Nineth Conference on Severe Local Storms* (Norman, Oklahoma, 1975), p. 371-372.

Ibid., 371.

*light detection and ranging

particles within the tornado, and return to a coaxially mounted detector with enough detectable signal to allow synthesis of the frequency spectra, 2) to determine which wavelength(s) is(are) the most conducive to this type of analysis, and 3) to determine the optimum pulse width required to obtain the desired spectra. The resultant spectra may then be analyzed to obtain the Doppler shifts and thence the velocities of the turbulence.

Basic Assumptions

The following assumptions served as a foundation for the calculations and results of this investigation.

1. The tornado emanates from a cloud structure and, until it contacts the ground, it will maintain the particulate composition of the generating cloud.

2. The cloud composition consists of particles ranging in size from less than 1 μm to about 25 μm with mode radius of the order of several micrometers and concentrations which depend upon the type of cloud considered.

3. The three models used as test distributions approximate extreme conditions of cloud composition (relative to tornado-type turbulence).

4. The particles within the cloud are spherical and partially absorbing. (And thus the scattering which predominates is commonly referred to as Mie scattering.)

5. The scattering that occurs from a particular particle is independent of the scattering from other particles in the cloud.

6. The effects of multiple scattering can be neglected in determining the properties of extinction and backscatter.

CHAPTER II

THEORETICAL BACKGROUND

Laser Propagation in the Atmosphere

The propagation of light emitted into the atmosphere by a laser is unique in that it is highly directional and very nearly monochromatic. In addition, a laser beam has a high degree of both spatial and longitudinal coherence (coherence times can be on the order of 10^{-2} seconds) and radiates as a gaussian-spherical light beam (spherical waves having a gaussian variation in amplitude across the wavefront).[1,2] This light beam may be unpolarized, plane-polarized, or elliptically-polarized as desired.

An optical wave, propagating in the z-direction with frequency, ω, may be represented mathematically as

$$\phi(x,y,z,t) = E'(x,y)e^{i(\omega t - kz)} \quad \text{(volts/meter)}$$

where $E'(x,y)$ is the complex wave amplitude whose (normalized for unit power flow) form is

$$E'(x,y) = \left(\sqrt{\frac{2}{\pi}}\right) \frac{2}{W} \exp\{-i \frac{\pi}{\lambda} \frac{x^2+y^2}{R}\} \exp\{-\frac{x^2+y^2}{W^2}\} \quad \text{(volts/meter)}$$

---

[1]A. E. Siegman, *An Introduction to Lasers and Masers* (New York: McGraw-Hill Co., 1971) 306.

[2]R. S. Longhurst, *Geometrical and Physical Optics* (3rd ed., London: Longman Group Limited, 1973) pp. 111-113.

with R representing the radius of curvature of the spherical wave and W the beam radius.[3]

One may apply far-field diffraction theory to this wave and obtain expressions for the far-field spot size, radius of curvature and the diffraction angle. These expressions are, respectively,

$$W(Z) = W(o)\sqrt{1+\left(\frac{\lambda Z}{\pi W(o)^2}\right)^2} \simeq \frac{\lambda Z}{\pi W(o)} \text{ (meters); } Z >> \frac{\pi W(o)^2}{\lambda} \qquad (1\text{-}2a)$$

$$R(Z) = Z[1+(\pi W(o)^2/\lambda Z)^2] \simeq Z \text{ (meters); } Z >> \frac{\pi W(o)^2}{\lambda} \qquad (1\text{-}2b)$$

$$\Theta = W(Z)/R(Z) \simeq \lambda/\pi W(o) \text{ (radians); } Z >> \frac{\pi W(o)^2}{\lambda} \qquad (1\text{-}2c)$$

where these expressions have been derived on the basis of a '1/e' criteria and will thus contain about 86 per cent of the full gaussian beam. Note that the laser beam does not lose its spherical-gaussian nature when transmitted through an optical lens.[4,5]

In order to achieve a significant amount of backscatter at the distances involved, one must have an appreciable scattering area. Being cognizant of the further requirement that one of the objects of this study is to localize the area of the tornado from which we wish to obtain the data, we arbitrarily selected a scattering area of 10 m^2 as a starting point. Relating this to the beam

---

[3]A. E. Siegman, *An Introduction to Lasers and Masers*, p. 307.

[4]*Ibid.*, 308-309, 315.

[5]F. P. Gagliano and U. J. Zaleckas. "Laser Processing Fundamentals." *Lasers in Industry*. Edited by S.S. Charschan. New York: van Nostrand Reinhold Company, 1972.

radius, we have, at the scattering area, a beam radius of about 1.78 m. Using the above expressions we obtain a spot size at the transmitter on the order of 2 cm for a beam of wavelength 10.6 μm. Using a typical beam waist (of a 10.6 μm laser) of about 5.0 mm we require optical magnification of about 4X at the transmitter to achieve the desired scattering area.

The intensity of our optical wave is given by the expression

$$I = \phi\phi^* = E'(x,y)E'^*(x,y) = \frac{8}{\pi W^2} \exp\left\{-\frac{2(x^2+y^2)}{W^2}\right\} \quad \text{(watts)} \qquad (1\text{-}3)$$

However, we are primarily interested in the ratio of the emitted intensity to the received intensity. This expression is derived from consideration of the elements involved; those dictated by the field of view of the detector, the medium through which the beam travels, and the scattering volume itself. For a diffraction-limited detector, the field of view, Ω, is given by

$$\Omega = \lambda^2/A_d \quad \text{(steradians)} \qquad (1\text{-}4)$$

where λ is the wavelength of the beam and A_d is the capture area of the detector.

The medium in this case is the atmosphere between the transceiver and the tornado and it is characterized by a transmissivity, τ_A, which is dependent upon the constituents of the atmosphere. This transmissivity will be discussed in detail shortly, but for our purpose here we shall consider it as a multiplicative

constant. The scattering volume is accounted for in the following manner: The back-scattered radiation is dependent on the physical dimensions of the scattering volume, the transmissivity, τ_s, and the volume back-scattering function, $\beta(\pi)$, of the volume irradiated. We have selected a scattering area, A, of $10m^2$. The length of the scattering volume, L, is in principle, a function of the width of the pulse. The transmissivity is again dependent upon the constituents of the scattering volume and is given by the expression

$$\tau_s = \exp\{-\beta_{ext}L\} \quad \text{(dimensionless)} \qquad (1\text{-}5)$$

where β_{ext} is the extinction coefficient derived from the Mie theory and L is as defined above. The volume back-scattering function, $\beta(\pi)$, is also computed from the Mie theory. Details for deriving $\beta(\pi)$ and β_{ext} are given later.

We can summarize the above discussion with the following relation, noting that the radiation must traverse the path in both directions,

$$I_{RECEIVER} = H(\lambda)AL\Omega\tau_A{}^2\beta(\pi)\exp\{-2L\beta_{ext}\} \quad \text{(watts)} \qquad (1\text{-}6)$$

where $H(\lambda)$ is the spectral irradiance in watts/m^2 and the other quantities are as discussed above.[5]

The field of view for a diffraction-limited detector is given in Table I for appropriate values of wavelength using a 15.24 cm diameter lens for the aperature.

---

[5]D. B. Rensch and R. K. Long. "Comparative Studies of Extinction and Backscattering by Aerosols, Fog, and Rain at 10.6 and 0.63 μ", *Applied Optics 9*, No. 7 (July, 1970) p. 1563.

Table 1. Field of View for a 15.24 cm, Diffraction-Limited Detector at Various Wavelengths.

Wavelength (Micrometers)	Field of View (Steradians)
10.6	0.616×10^{-9}
4.0	0.877×10^{-10}
1.06	0.616×10^{-11}
0.5	0.137×10^{-11}

Atmospheric Attenuation

Given this pulsed laser signal emanating from the transmitter into the atmosphere towards the tornado, we seek to derive an expression for the attenuation of the signal by the intervening medium and the turbulence itself. This attenuation is a function of the nature of the medium; the molecular constituents and aerosols (dust, smoke, carbon particles, etc.) present under any given circumstance. For most conditions, the attenuation assumes an exponential form given by an extension of the Lambert-Beers law:

$$\tau_A = \exp\{-\alpha L\} \quad \text{(dimensionless)}$$

where τ_A is the atmospheric transmissivity, α is the attenuation or extinction coefficient, and L is the path length. In the type of media commonly referred to as normal or clear air atmosphere, the attenuation coefficient is composed of four parts, i.e.,

$$\alpha = \sigma_a + \kappa_a + \sigma_b + \kappa_b \qquad (\text{length})^{-1}$$

where σ, and κ denote scattering and absorption, respectively. The subscripts a and b refer to aerosol and molecular effects, respectively.[6] Of these four parts, only two have significant bearing for the wavelengths we are considering in this research; these are molecular absorption and aerosol scattering. Molecular scattering and aerosol absorption prove to be negligible in comparison.

---

[6]Paul W. Kruse, Laurence D. McGlauchlin, and Richard B. McQuistan. *Elements of Infrared Technology* (New York: John Wiley & Sons, Inc., 1962), p. 162-192.

For molecular absorption, the components of consequence are generally considered to be water vapor (H_2O), carbon dioxide (CO_2), and ozone, but the latter is dropped for two reasons: the ozone concentration at the altitudes we are interested in (sea level to 12 kilometers) is negligible and the absorption coefficient for wavelengths of 0.90 μm and above is zero.[7,8] N_2 and O_2, which together account for about 98 per cent of the volume, do not exhibit absorption bands since, being homonuclear, they do not possess either a permanent or induced electric moment. To minimize the effect of molecular absorption, one must avoid the sharp absorption bands associated with water vapor (1.1 μm, 1.38 μm, 1.87 μm, 2.7 μm, and 6.0 μm) and with CO_2 (2.7 μm, 4.3 μm, and 14.5 μm). If these bands are avoided, the transmissivity will be significantly greater.[9]

Molecular scattering (Rayleigh scattering) is negligible in our case as may be seen from the following considerations: the molecular diameters of the most prevalent constituents of the atmosphere are all on the order of a few angstroms (10^{-10} meters).[10] The attenuation coefficient may be ascertained by the following formula:

---

[7]William K. Pratt. *Laser Communication Systems* (New York: John Wiley & Sons, Inc., 1969), p. 129.

[8]Louis Alterman and Robert B. Tollin. "Atmospheric Optics," *Handbook of Geophysics and Space Environments*, Ed. Shea L. Valley (New York: McGraw-Hill Co., 1965), p. 7-30.

[9]Kruse, *Elements of Infrared Technology*, pp. 163-164.

[10]Robert C. Weast. Ed., *Handbook of Chemistry and Physics* (54th Ed.,; Cleveland: CRC Press, 1973), p. F191.

$$\sigma_b = 0.827\ N\ A_p{}^3\lambda^{-4} \quad (\text{length})^{-1}\ , \qquad (2\text{-}1)$$

where n is the number of particles per unit volume in the path, A_p is the cross sectional area of the scatter (a fraction of the circular cross-section), and λ is the wavelength of the incident light.[7] This formula yields an attenuation coefficient on the order of 10^{-2} for circular cross sections. The listed value of the attenuation coefficient for 0.5 μm is 1.716×10^{-2} km^{-1}; in comparison, the listed value of attenuation coefficient for aerosols at 0.5 μm is 0.167 km^{-1} and therefore the molecular scattering is about 10 per cent at this wavelength.[8] As wavelength increases, σ_b decreases as the fourth power while σ_a decreases only by an order of magnitude (as will be shown directly) in the range from 0.50 μm to 10.6 μm. Thus we neglect the attenuation due to molecular scattering at these wavelengths in the normal, clear air atmosphere.

Aerosol attenuation in the atmosphere may be described by the Mie theory. Due to the particular nature of the aerosols, aerosol absorption is again neglected (as it is small in comparison

---

[7]Pratt, *Laser Communication Systems*, p. 131.

[8]Elterman and Tollin, *Handbook of Geophysics and Space Environments*, pp. 7-30.

tothe effect of scattering) and an empirical relationship, based on this theory, has been derived which gives good results for clear air scattering. This relationship is:

$$\sigma_a = \frac{3.91}{V} \left[\frac{\lambda}{0.55}\right]^{-0.585V^{1/3}} \quad \text{(kilometers)}^{-1} \quad (2\text{-}2)$$

where V is the visual range in kilometers.[11] However, this formula should be regarded as a minimum since it does not include variations in local meteorological conditions. A review of representative values for the aerosol attenuation coefficient indicates variation in values of almost twice that given by Equation (2-2) for 1.06 μm, over five times greater for 4 μm and almost thirteen times greater for 10.6 μm.[12] Table 2 reflects these variations for a visibility of 10 km. Similarly, local meteorological conditions affect molecular absorption. A variation in the atmospheric absorption of CO_2 of 0.08db/km between January and July has been reported by Yin and Long for a wavelength of 10.6 μm.[13] Water vapor absorption is a function of the water-vapor concentration which in turn depends on both relative humidity and temperature. The figures for molecular absorption in Table 2 have been obtained using concentrations of CO_2 and water vapor of 700 atm-cm and 15.0 precipitable-cm respectively, in

---

[11] Kruse, *Elements of Infrared Technology*, p. 191.

[12] Douglas P. Woodman. "Limitations in Using Atmospheric Models for Laser Transmission Estimates." *Applied Optics 13:10*, 2193 (October, 1974).

[13] P.K.L. Yin and R. K. Long. "Atmospheric Absorption at the Line Center of P(20) CO_2 Laser Radiation." *Applied Optics 7:8*, 1551 (August, 1968).

the transmission tables of Wyatt, Stull and Plass.[14,15,16] The CO_2 concentration, atmosphere-centimeter is defined as "... the length in centimeters of a column whose volume would contain the same number of molecules of CO_2 gas at NTP as a column of the same cross section, but of arbitrary length, pressure, and temperature." The H_2O concentration, precipitable-centimeters, is defined as "...the thickness of the liquid that would be formed if all the water vapor traversed by a beam of uniform cross section were completely condensed in a container of cross section equal to that of the beam."[14] The 700 atm -cm/km gives a CO_2 absorption coefficient equivalent to 0.3 db/km, which is consistent with the data of Yin and Long. The 15.0 precipitable-cm/km corresponds to the data achieved by McCoy, Rensch, and Long.[17] The values in Table 2 seem to cover most of the published values for the effects noted; however, it is stressed that local meteorological conditions will change these figures, especially those of water vapor absorption.

---

[14]John N. Howard, John S. Garing, and Russell G. Walker. "Transmission and Detection of Infrared Radiation." *Handbook of Geophysics and Space Environments.* Edited by Shea L. Valley, New York: McGraw-Hill Co., 1965.

[15]Philip J. Wyatt, Robert V. Stull, and Gilbert N. Plass. "The Infrared Transmittance of Water Vapor." *Applied Optics 3:2,* 229 (February, 1964).

[16]Philip J. Wyatt, Robert V. Stull, and Gilbert Plass. "The Infrared Tramsmittance of Carbon Dioxide." *Applied Optics 3:2,* 243 (February, 1964).

[17]John H. McCoy, David B. Rensch, and Ronald K. Long. "Water Vapor Continuum Absorption of Carbon Dioxide Laser Radiation Near 10μ." *Applied Optics 8:7,* 1471 (July, 1969).

Table 2. Transmission Loss of the Intervening Atmosphere.

Wavelength (micro-meters)	Aerosol Scattering (db/km)	Molecular Absorption (db/km)		Transmission Loss (db/km)
		CO_2	H_2O	
10.6	.04-.49	0.3	1.6	1.94-2.39
4.0	.14-.75	2.16	1.0	3.30-3.91
1.06	.74-1.44	0.0	0.09	0.83-1.53
0.5	1.91-2.14	0.0	0.0	1.91-2.14

Mie Scattering Theory

Scattering theory has developed as a natural outgrowth of the study of light. As such, it was greatly influenced by Maxwell's electromagnetic theory of light. Mie solved Maxwell's equations for various types of homogeneous spheres using approximate boundary conditions. The full details may be found in the original paper published in 1908 (*Ann. Physik 25*, 377). A concise outline is found in many books including van de Hulst. The Mie solution is considered the analytical solution as it is a formal, mathematical analysis of scattering from a sphere. It is applicable to all sizes of spheres and uses a size parameter, $x = kr = 2\pi r/\lambda$, where r is the radius of the sphere and λ the wavelength of the incident light. Several approximations have been developed including the two extremum approximations, the Rayleigh (scattering) approximation ($x \ll 1$) and geometrical optics ($x \to \infty$). The Mie solutions confirm these approximations which in turn, are normally used in lieu of the Mie solutions simply because of the computational analysis involved with the latter. However, no acceptable approximation has been developed for the size range we are investigating ($x \approx 1$) so we adopt the Mie solution and proceed.

The results of a single, independent scattering process of a scalar wave may be generally expressed in the following manner:

$$\begin{pmatrix} E_{\parallel} \\ E_{\perp} \end{pmatrix} = \begin{pmatrix} S_2 & S_3 \\ S_4 & S_1 \end{pmatrix} \frac{e^{-ikr+ikz}}{ikr} \begin{pmatrix} E_{\parallel} \\ E_{\perp} \end{pmatrix}_o \quad \text{(volts/meter)} \qquad (2\text{-}3)$$

where the S_i are amplitude functions dependent upon θ and ϕ, the angle

between the directions of propagation of the incident light and the scattered light and the azimuthal angle respectively; $E_{\parallel}$ and $E_{\perp}$ are the electric field components parallel to and perpendicular to the direction of propagation, z; $\vec{r}$ is the radial vector perpendicular to z; and k is the propagation constant. For spherical scatterers, S_3 and S_4 are zero, so one of our primary objectives is to obtain S_1 and S_2.

They have been derived by applying boundary conditions to the general solutions of the scalar wave equation in polar coordinates. Noting that our interest in the scattered wave is in the far field, approximations for the spherical Bessel functions are applicable. The resulting normalized components of the electric and magnetic fields, are (using polar notation)

$$E_\theta = H_\phi = -\frac{i}{kr} e^{-ikr+i\omega t}(\cos\phi)S_2(\theta) \quad \text{(dimensionless)} \quad (2\text{-}4a)$$

$$-E_\phi = H_\theta = -\frac{i}{kr} e^{-ikr+i\omega t}(\sin\phi)S_1(\theta) \quad \text{(dimensionless)} \quad (2\text{-}4b)$$

$$S_1(\theta) = \sum_{n=1}^{\infty} \frac{2n+1}{n(n+1)} [a_n \pi_n(\cos\theta) + b_n \tau_n(\cos\theta)] \quad \text{(dimensionless)} \quad (2\text{-}5)$$

$$S_2(\theta) = \sum_{n=1}^{\infty} \frac{2n+1}{n(n+1)} [b_n \pi_n(\cos\theta) + a_n \tau_n(\cos\theta)] \quad \text{(dimensionless)} \quad (2\text{-}6)$$

where ω = circular frequency (radians/sec),

$$\pi_n(\cos\theta) = \frac{1}{\sin\theta} P_n^1(\cos\theta) ,$$

$$\tau_n(\cos\theta) = \frac{d}{d\theta} P_n^1(\cos\theta) ,$$

$P_n^1(\cos\theta)$ = Bessel functions

and a_n and b_n are known as the (complex) Mie coefficients which are

dependent upon the complex index of refraction, m, and the size parameter, x.[18] They may be expressed most compactly in terms of the Ricatti-Bessel functions, $\Psi_n(x)$ and $\xi_n(x)$, they are,

$$a_n = \frac{A_n(y)\Psi_n(x) - m\Psi_n'(x)}{A_n(y)\xi_n(x) - m\xi_n'(x)} \qquad \text{(dimensionless)}$$

$$b_n = \frac{mA_n(y)\Psi_n(x) - \Psi_n'(x)}{mA_n(y)\xi_n(x) - \xi_n'(x)} \qquad \text{(dimensionless)}$$

where,

$$y = mx$$

$$A_n(y) = \frac{\Psi_n'(y)}{\Psi_n(y)}$$

$$\Psi_n'(x) = \frac{d}{dx}\Psi_n(x)$$

$$\xi_n'(x) = \frac{d}{dx}\xi_n(x)$$

$$\Psi_n(x) = \sqrt{\frac{\pi x}{2}}\, J_{n+\frac{1}{2}}(x)$$

$$\xi_n(x) = \sqrt{\frac{\pi x}{2}}\, [J_{n+\frac{1}{2}}(x) + i(-1)^n J_{-n-\frac{1}{2}}(x)] \quad .[18,19]$$

(all dimensionless)

---

[18] H. C. van de Hulst. *Light Scattering by Small Particles.* New York: John Wiley & Sons, Inc., 1957.

[19] D. Deirmendjian. *Electromagnetic Scattering on Spherical Polydispersions.* New York: American Elsevier Publishing Company, Inc., 1969.

At this point, we can determine the nature of the electromagnetic fields of an incident beam scattered from a homogeneous sphere of radius, r, at an angle, θ, from the incident beam and at an azimuthal angle, ϕ. Furthermore, with the additional assumptions of single and independent scattering, we can apply the results to N particles of radius, r, by simply invoking the principle of superposition and adding the contributions from each particle. Maintaining these assumptions, we can also extend the theory to include a distribution of particles by computing the Mie amplitude factors and coefficients of each representative particle and summing the resultant contributions weighted by their relative occurrence in the distribution. In these cases, we must extend the notation of the $S_i(\theta)$ to include the functions of x and m, $S_i(\theta)$ becomes $S_i(x,m,\theta)$.

There is a further aspect we have not addressed explicitly as yet and that is, the extent to which the incident light is scattered and/or absorbed. As intimated earlier in the case of molecular scattering, only a fraction of the incident light is scattered and/or absorbed. The fraction that is scattered (absorbed) is equivalent to the scattering (absorption) cross section divided by the geometrical cross section. It is referred to as the scattering (absorption) efficiency factor, $K_{sc}(K_{abs})$, (the K is replaced by a Q in van de Hulst's notation). Another convenient parameter is the total extinction efficiency factor, K_{ext}, which is the algebraic sum of the scattering and absorption efficiencies. K_{sc} and K_{ext} may be derived from the integration of the Mie amplitude functions Equations (2-5) and (2-6) and are given by

$$K_{sc}(x,m) = \frac{2}{x^2} \sum_{n=1}^{\infty} (2n+1)(|a_n|^2+|b_n|^2) \qquad \text{(dimensionless)} \qquad (2\text{-}7)$$

$$K_{ext}(x,m) = \frac{2}{x^2} \sum_{n=1}^{\infty} (2n+1)\mathrm{Re}\{a_n+b_n\} . \qquad \text{(dimensionless)} \qquad (2\text{-}8)$$

Equations (2-5) through (2-8) are considered the fundamental parameters of the Mie Theory, as all the other parameters required to describe the intensity and polarization of scattered light may be derived from these four parameters.[20]

We are now in a position to describe those functions previously referred to as the extinction coefficient, β_{ext}, and the volume backscattering function, $\beta(\pi)$. These functions are determined from the particle size distribution, $n(r)$, the scattering efficiency and as yet undefined quantities known as the Mie intensity functions, i_j, which are derived from the amplitude functions Equations (2-5) and (2-6) by means of the traditional method of obtaining intensities from amplitudes, that is

$$i_1(x,m,\theta) = S_1S_1^* \qquad \text{(dimensionless)}$$

$$i_2(x,m,\theta) = S_2S_2^* \qquad \text{(dimensionless)}$$

For a single particle, β_{ext} is just the extinction cross section, but for a distribution of particles, β_{ext} must include the contributions from all particles. Therefore we once again apply the principle of superposition and, expressing β_{ext} in terms of the parameter x,

---

[20] *Ibid.*, p. 74.

$$\beta_{ext} = C\int_{x_{min}}^{x_{max}} n(x)x^2K_{ext}(x,m)dx \quad (length)^{-1} \tag{2-9}$$

where C is the constant obtained when converting n(r) and r to n(x) and x respectively.[21]

Similarly, $\beta(\pi)$ is found to be

$$\beta(\pi) = \sum_{j=1}^{2} D\int_{x_{min}}^{x_{max}} n(x)i_j(x,m,\pi)dx \quad (length)^{-1}(steradian)^{-1}$$

where D is the constant which includes the conversion factors. This can be further simplified by noting that $i_1 = i_2$ for $\theta = \pi$ so that

$$\beta(\pi) = D'\int_{x_{min}}^{x_{max}} n(x)\, i_1(x,m,\pi)dx \quad (length)^{-1}(steradian)^{-1}.[22] \tag{2-10}$$

We now proceed to describe the distribution function n(r) which specifies concentration, mode radius and shape of the curve depicting the particles in our scattering volume.

The Distribution Function

Precipitating clouds have characteristics which vary widely depending on the location, humidity and other conditions. Our procedure was to select clouds associated with tornadoes in the local area (Oklahoma), determine the characteristics of these clouds, and

---

[21] *Ibid.*, p. 14.

[22] *Ibid.*, pp. 89, 119.

then proceed to obtain distribution functions which closely match those characteristics.

The local continental clouds are believed to have the following characteristics: (1) The concentration in the funnel cloud has a maximum near 1000 particles/cm^3 and a minimum of about 150 particles/cm^3. (2) The mode radii associated with the above concentrations are 5 μm and 15 μm respectively. (3) The relative dispersion, D_b = (the standard deviation of particle radii)/(mode particle radius), on the order of 0.366. And, (4) The significant portion of the particles being in the range of 1 μm to 25 μm in radius.[23,24]

The distribution function used was first proposed by Deirmendjian and has since been used by several investigators in similar applications.[25,26,27] Selected on the basis of its versatility and relation to physical interpretation, that function is,

$$n(r) = ar^{\alpha}\exp(-br^{\gamma}) \quad cm^{-3}/\mu m \quad 0 \leq r \leq \infty \qquad (2\text{-}11)$$

where the four constants a, b, α, γ are real and positive, and α is

---

[23]Joanne Simpson and Victor Wiggert. "Models of Precipitating Cumulus Towers." *Monthly Weather Review 97:7*, 471 (July, 1969).

[24] John McCarthy. Personal Interview. September, 1975.

[25] D. Deirmendjian. *Scattering and Polarization Properties of Polydispersed Suspensions with Partial Absorption.* Report prepared for United States Air Force Project Rand, Memo# RM-3228-PR, July, 1962. Santa Monica, CA:Rand Corporation, 1962.

[26]R. C. Anderson and E. W. Browell. "First- and Second-Order Backscattering from Clouds Illuminated by Finite Beam." *Applied Optics 11:6*, 1345 (June, 1972).

[27] D. B. Rensch and R. K. Long. "Comparative Studies of Extinction and Backscattering by Aerosols, Fog, and Rain at 10.6μ and 0.63μ." *Applied Optics 9:7*, 1563 (July, 1970).

an integer. Further properties are noted by Deirmendjian in the original work and in his book (Deirmendjian, 1969); however, only the values of the constants concern us here. α and γ are obtained, in our case, by trial and error to fit the relative dispersion, D_b, and the estimated range of the particles. "b" is obtained by differentiating n(r) with respect to r and determining the absolute maximum; it is given by,

$$b = \frac{\alpha}{\gamma r_c^{\gamma}} \quad (\mu m)^{-\gamma} \tag{2-12}$$

where r_c is the mode radius of the distribution. "a" is obtained by integrating n(r) over the range of r and solving for a particular value of N, the concentration of particles. Thus, a is given by

$$a = \frac{N\gamma b^{(\alpha+1)/\gamma}}{\Gamma(\alpha+1/\gamma)} \quad (\text{particles/cm}^3)(\mu m)^{-(\alpha+1)} \tag{2-13}$$

where $\Gamma(x)$ is the gamma function.[28]

Doppler Effect

To determine the velocity of the particles from which the incident light beam is scattered one applies the principle of the Doppler effect. To be precise, one would use the precepts of the Theory of Special Relativity to obtain the frequency shift and thence the velocity. For incident light with frequency f, the expression for the Doppler-shifted frequency f' is

---

[28]Deirmendjian, *Scattering and Polarization*, pp. 2-3.

$$f' = \left(\frac{1\mp\beta}{1\pm\beta}\right)^{\frac{1}{2}} f \quad \text{Hz}$$

where β = velocity of particle/speed of light = v/c and the top sign is used for motion away from the observer while the bottom sign is used for motion toward the observer.[29] However, we are dealing with velocities on the order of 100 m/sec so we use the first-order approximations of

$$f' = \frac{f}{1\pm\beta} = \frac{f}{1\pm v/c} \quad \text{Hz}$$

we must also account for the direction of the velocity of the particle in relation to the receiver since it is the velocity component in the direction of the receiver that accounts for the change in the frequency. Then, one obtains

$$f' = \frac{f}{1 \pm \frac{v}{c}\cos\theta} \quad \text{Hz} \qquad (2\text{-}14)$$

where θ is the angle between the direction of the particle and the receiver as in the sketch below.[30]

---

[29] A. P. French. *Special Relativity*. New York: W. W. Norton and Co., Inc., 1968.

[30] F. P. Gagliano and U. J. Zaleckas. "Laser Processing Fundamentals." *Lasers in Industry*. Edited by S. S. Charschan. New York: Van Nostrand Reinhold Company, 1972.

To determine the velocity resolution of the laser, we must take into consideration the spectral width, S_B, of the laser since a laser does not emit radiation of a single frequency. We proceed as follows: A reasonable velocity resolution of 1m/sec is consistent with the total velocities within a tornado. Using Equation (2-14) and assuming a velocity component, $v_o (= v\cos\theta)$, approaching the receiver we obtain for v_o,

$$v_o = (1 - \frac{f}{f'})c = \frac{f'-f}{f'} c \cong \frac{S_B/2}{f'} c \qquad \text{(meter/sec)}$$

To obtain a 1m/sec velocity resolution we must have for a wavelength of 10.6 μm, $S_B = \frac{2v \cdot f}{c} = \frac{2(1\text{m/sec})2.83\times10^{13}/\text{sec}}{3\times10^{8}\text{m/sec}} = 1.887\times10^{5}$ Hz. One similarly obtains maximum spectral widths of 5×10^5 Hz, 1.887×10^6 Hz, 4×10^6 Hz for the wavelengths of 4 μm, 1.06 μm, and 0.5 μm, respectively. According to De Nicola, these spectral widths are well within the capabilities of today's lasers.[31]

The bandwidth of the receiver is also affected by the velocity of the particle; in this case it is the maximum expected velocity of 100m/sec. Applying the above principles, we obtain receiver bandwidths of 1.887×10^7 Hz, 5×10^7 Hz, 1.887×10^8 Hz, and 4×10^8 Hz for wavelengths of 10.6 μm, 4 μm, 1.06 μm, and 0.5 μm, respectively.

A consequence of this discussion is based on the inherent property of the Doppler effect to account for the velocity component of the particle parallel to the direction of the receiver. Thus maximum velocity spectra will come from the side portions of the turbulence.

---

[31] R. O. DeNicola. "Reflection and Scattering," *Lasers in Industry*. S. S. Charschan (New York: Van Nostrand Reinhold Co., 1972).

Heterodyne Detectors

To detect the backscattered radiation, we propose a coaxially mounted, heterodyne detector. A coaxial mount takes full advantage of the backscattered radiation, and heterodyning is desirable for a variety of reasons which include, high sensitivity, inherent narrowband detection and the wide range and availability of solid state detectors (with their higher quantum efficiencies) in the infrared region.[32] A further advantage of heterodyning is that, as will be shown, one can effectively eliminate the background, shot and thermal noise by controlling the local oscillator power.

The essence of heterodyning is depicted in Figure 1. The signal current, i_{sig}, is given by the product of the detector proportionality constant, $\beta = q\eta/hf_s$, (the responsivity) the gain, G, and the total signal squared (assuming square law detection). The result is, assuming $\Delta\omega << \omega_o$, ω_s, and that the detector is unable to follow the fast variations in frequency,

$$i_{sig} \simeq \beta G\left(\frac{E_s^2}{2} + \frac{E_o^2}{2} + E_s E_o \cos\Delta\omega t\right) \quad \text{(Amperes)}$$

eliminating the dc terms, the power delivered to the load resistor, R_L, is

$$S = i_{sig}^2 R_L = \frac{G^2\beta^2 E_s^2 E_o^2 R_L}{2} \quad \text{(watts)}$$

or, in terms of the average power,

$$S = 2G^2\beta^2 P_s P_o R_L \quad \text{(watts)} \text{ .}^{33} \quad (2\text{-}15)$$

---

[32] S. S. Charschan. "Detection and Measurement," *Lasers in Industry* (New York: Van Nostrand Reinhold Co., 1972).

[33] Pratt, *Laser Communication Systems*, p. 187.

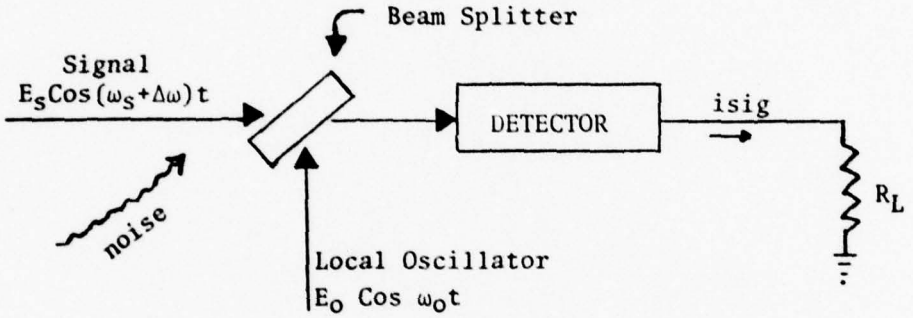

Figure 1. Basic Heterodyne Detector.

The total noise delivered to the load resistor primarily arises from five sources which manifest themselves as shot noise and thermal noise. The shot noise is comprised of the following: the dark current, I_D, and the currents generated by fluctuations in the background radiation, the local oscillator and the carrier itself. Included in this type of noise may be the generation-recombination noise for photovoltaic and photoconductive detectors. The thermal noise is the familiar Johnson or Nyquist thermal noise. The total expression for noise in terms of the average power is

$$N_{IF} = 2G^2q[\beta(P_s+P_o+P_B)+I_D]B_{IF}R_L + 4kTB_{IF} \text{ (watts)}$$

where P_S, P_O, P_B represent the signal, oscillator, and background noise respectively, k is Boltzmann's constant, T is the temperature in degrees Kelvin, and B_{IF} is the bandwidth of the IF filter.[34] As stated, making the power of the local oscillator large with respect to the other parameters tends to make those other parameters negligible and

$$N_{IF} = 2G^2q\beta P_oR_LB_{IF} \text{ .} \qquad \text{(watts)} \qquad (2\text{-}16)$$

Combining Equations (2-15) and (2-16) we obtain for the signal to noise ratio (SNR)

$$\left(\frac{S}{N}\right)_{IF} = \frac{2G^2\beta^2P_sP_oR_L}{2G^2q\beta P_oR_LB_{IF}} = \frac{\beta P_s}{qB_{IF}} = \frac{\eta P_s\lambda}{hcB_{IF}} \quad \text{(dimensionless)}$$

which becomes, for a sine wave plus narrow-band Gaussian noise input, using the square law detector,

---

[34] *Ibid.*, 187.

$$\frac{S}{N} = \frac{\eta P_s \lambda}{2hcB_{IF}} \quad \text{(dimensionless)} \qquad (2\text{-}17)$$

[35]

Now, $B_{IF} \geq 2B_s$ and so, to accommodate the Doppler shift as previously discussed, the SNR will be slightly lower. If homodyne detection is used, the bandwidth of the local oscillator will have to be extended similarly for the doppler effect.

As a minimum, the SNR should equal unity, so we may calculate the required signal power from Equation (2-17) using the receiver bandwidths calculated in the previous section. We obtain, for a quantum efficiency, n, of 1, and a wavelength of 10.6 μm,

$P_s = 2B_{IF}hf = 4B_s hf = 4(1.887\times10^{7}\ \text{sec}^{-1})(6.626\times10^{-34}\ \text{joule-sec})(2.83\times10^{13}\ \text{sec}^{-1}) = 1.41\times10^{-12}$ watts. Similarly, we obtain minimum signal powers of 9.94×10^{-12} watts, 1.41×10^{-10} watts, and 6.36×10^{-10} watts for the wavelengths of 4.0 μm, 1.06 μm, and 0.5 μm, respectively.

Ross notes that "...communications would be difficult at SNR = 1 and hence at least a factor of ten is required for adequate communication."[36] Therefore, our signal powers should be an order of magnitude larger than the minimum computed above.

---

[35] *Ibid.*, pp. 187-190.

[36] Monte Ross. *Laser Receivers* (New York: John Wiley and Sons, Inc., 1966), p. 327.

CHAPTER III

PROCEDURES AND CALCULATIONS

Computer Implementation

The use of a computer to develop the Mie parameters and analyze the scattering of light from a distribution of particles is a necessity due to the infinite series involved. There are tables available that list the Mie parameters [see (Deirmendjian, 1963) for example and (van de Hulst,1957) for a representative listing of various sources]. However, the tables are unsuitable for some applications due to truncation of the values or to interval spacing which is too large for present day applications as noted for example, in works by Dave.[1,2]

The Mie parameters are quite adaptable to computerization as has been shown by Dave.[3] We used the adaptations of Deirmendjian

---

[1]J. V. Dave. "Effect of Coarseness of the Integration Increment on the Calculation of the Radiation Scattered by Polydispersed Aerosols." *Applied Optics 8:6*, 1161 (June, 1969).

[2]J. V. Dave. "Effect of Varying Integration Increment on the Computed Polarization Characteristics of the Radiation Scattered by Polydispersed Aerosols." *Applied Optics 8:10*, 2153 (October, 1969).

[3]J. V. Dave. "Subroutines for Computing the Parameters of the Electromagnetic Radiation Scattered by a Sphere." Report prepared for IBM, Rep. 320-3237. Palo Alto, CA: IBM Scientific Center, 1968.

(see Appendix A) to determine the fundamental Mie parameters as specified in Equations (2-5) through (2-8). The interval spacing was approximately 0.25 μm. Using this interval, we proceeded to compute the distribution function, n(x) and ultimately the extinction coefficient, β_{ext}, and the volume backscattering function, $\beta(\pi)$, using numerical integration (trapezoidal rule) for all the distributions. The program then computes the received intensity (neglecting atmospheric transmission effects) as given by Equation (1-6), for one-meter increments of the length of the scattering volume.

Appendix B has a flowchart of the computer program. It is not all inclusive, but is given as an aid in deciphering the program. Appendix C has the complete computer program printout. For simplicity, it is written in the Fortran Language, using a WATFIV compiler.

Programming the Mie Parameters

The calculations proceed in the following manner: After initialization of the various parameters an "x-Do loop" is established for each required x. The end point values of x and the step size, Δx, are listed in Table 3 with their corresponding values of r and Δr for each wavelength considered. For each x, the initial values of A_o, W_{-1}, W_o are computed as A_2, W_1, W_2 respectively to avoid using negative and zero indices. A nested " -Do loop" is then created to compute the Mie functions W_n, π_n, τ_n, A_n, a_n and b_n and finally the Mie parameters $S_1(\pi)$ $[=S_2(\pi)]$, $K_{sc}(x,m)$, $K_{ext}(x,m)$ for values of n from 3 (corresponds to n = 1 as explained above) to a value n = 1.2 + 12.[4]

---

[4]D. Deirmendjian and R. J. Clasen. *Light Scattering on Partially Absorbing Homogeneous Spheres of Finite Size.* Report prepared for United States Air Force Project Rand, #R-393-PR, February, 1962. Santa Monica, CA: Rand Corporation, 1962.

Table 3. Distribution Endpoints and Stepsizes

λ(μm)	x_{min}, x_{max}	Δx	r_{min}, r_{max} (μm)	Δr(μm)
10.6	0.01,14.71	0.15	0.0169,24.82	0.253
10.6	0.01,14.71	0.30	0.0169,24.82	0.506
4.0	0.01,39.21	0.40	0.0064,24.96	0.255
4.0	0.01,39.01	0.75	0.0064,24.83	0.477
1.06	0.10,147.1	1.5	0.0169,24.82	0.253
0.5	0.10,311.95	3.15	0.008,24.82	0.251

This latter value is an iteration larger than that recommended by Deirmendjian to insure proper convergence of the finite series (after raising the indices). Larger numbers were tried but failed to alter the results, thus verifying the convergence. The "n-Do loop" ends after these iterations are complete for the named parameters.

Determining the Scattering and Extinction Properties

After computation of the Mie parameters, the extinction-, scattering-, backscatter-coefficients and the distribution functions, were computed for each x in intervals of Δx according to the following scheme: The form used for the extinction coefficient is

$$\beta_{ext} = \pi \int_{r_{min}}^{r_{max}} r^2 n(r) K_{ext}(m,x) dr \qquad (\text{length})^{-1}$$

To express this with one variable x, the variables r^2, $n(r)$, dr must be converted to expressions of the variable x.

$$r^2 = \left(\frac{x}{k}\right)^2 = \left(\frac{x\lambda}{2\pi}\right)^2 \qquad (\text{micrometers})^2$$

$$n(r) = n\left(\frac{x\lambda}{2\pi}\right) = a\left(\frac{x\lambda}{2\pi}\right)^{\alpha} \exp\left[-b\left(\frac{x\lambda}{2\pi}\right)^{\gamma}\right]$$

$$dr = \frac{\lambda}{2\pi} dx \quad . \qquad (\text{micrometers})$$

Therefore,

$$r^2 n(r) dr = \left(\frac{\lambda}{2\pi}\right)^{3+\alpha} a x^{\alpha+2} \exp\left[-b\left(\frac{\lambda}{2\pi}\right)^{\gamma} x^{\gamma}\right] dx$$

and,

$$\beta_{ext} = \pi\left(\frac{\lambda}{2\pi}\right)^{3+\alpha}(10^{-6})\int_{x_{min}}^{x_{max}} a x^{\alpha+2}\exp\left[-b\left(\frac{\lambda}{2\pi}\right)^{\gamma}x^{\gamma}\right]K_{ext}(m,x)dx \quad (\text{meter})^{-1}$$

which is in the form previously noted in Equation (2-9), the additional constant of 10^{-6} occurs due to changing the units so that β_{ext} is expressed in $(\text{meters})^{-1}$. Note that λ is expressed in microns. Similarly we find the expression for the scattering coefficient, β_{sc}, to be

$$\beta_{sc} = \pi\left(\frac{\lambda}{2\pi}\right)^{3+\alpha}(10^{-6})\int_{x_{min}}^{x_{max}} a\ x^{\alpha+2}\exp\left[-b\left(\frac{\lambda}{2\pi}\right)^{\gamma}x^{\gamma}\right]K_{sc}(m,x)dx$$

$$(\text{meter})^{-1}.$$

For the backscatter coefficient, we proceed along the same lines by starting with

$$\beta(\pi) = \pi\int_{r_{min}}^{r_{max}} r^2 n(r) K_b(m,x)dr \qquad (\text{length})^{-1}\text{-}(\text{steradian})^{-1}$$

where K_b, the backscattering efficiency, is defined as

$$K_b = \frac{4}{x^2}\left|S_1(\pi)\right|^2 \qquad (\text{dimensionless}).^5$$

Then we find, converting to the variable x as before, that

$$\beta(\pi) = \left(\frac{\lambda}{2\pi}\right)^{3+\alpha}(10^{-6})\int_{x_{min}}^{x_{max}} a x^{\alpha}\exp\left[-b\left(\frac{\lambda}{2\pi}\right)^{\gamma}x^{\gamma}\right]\left|S_1(\pi)\right|^2 dx$$

$$(\text{meter})^{-1}(\text{steradian})^{-1}.$$

---

[5] D. Deirmendjian. *Electromagnetic Scattering on Spherical Polydispersions*. New York: American Elsevier Publishing Company, Inc., 1969.

The "x Do-loop" continues with the computation of the summation terms for integration by the trapezoidal rule, which may be expressed in the following form:

$$\int_a^b f(x)dx = \frac{b-a}{n} \left[\tfrac{1}{2}f(a)+f(x_1)+f(x_2)+\cdots+f(x_{n-1})+\tfrac{1}{2}f(b)\right] \quad .^6$$

The program, as currently established, computes the integration for the extinction coefficient (BEXT 1,2,3,4), the scattering coefficient (BSC 1,2,3,4), and the backscatter coefficient (BPI 1,2, 3,4) for four different distribution functions and two different limits (each initiated at the same point, but having different maximums, LAST 1,2): The first set of limits was used for verification against known results for one of the distribution functions and the second set of limits was used for the set of distribution functions that represent the probable composition of the tornado funnel. In its present state, the program is easily rearranged to compute the coefficients mentioned in any combination of zero to four distribution functions in one set of limits with the remaining distribution functions in the second set of limits. In addition, one may easily expand (or contract) either the number of distribution functions or the number of sets of limits or the number of functions obtained by integration or all three. This is done, by adding the applicable distribution functions (FUN 5,6,...) and/or integration loops (BEXT 5,6,...; BSC 5,6,...; etc.), and then

---

[6]E. Kreyszig. *Advanced Engineering Mathematics.* 3rd Ed. New York: John Wiley and Sons, Inc., 1972.

adjusting the format statements for readout, to meet the specific need. The "x-Do loop" is completed by a printout of x and its associated Mie parameters at selected intervals of x.

Determining the Receiver Intensity

The program continues by computing the receiver intensity (Backscatter), as given by Equation (1-6) except for the transmissivity of the intervening atmosphere, for 1-meter increments of the length of the scattering volume (Resolution) for each distribution function, given a specific field of view and the area of the scattering volume (this quantity is entered as the single entity "OMEGA" in the program). [Appropriate controls have been entered here to keep from exceeding the negative exponential limit of the computer.]

The results currently programmed for printout are:
(1) x and its associated Mie parameters for selected intervals and (2) The extinction-, scattering-, and backscattering-coefficients together with the Resolution, solid angle (field of view--scattering area function, "OMEGA") and intensity ratio (Backscatter), for each distribution function identified with an index of J = 1,2,3, or 4.

The Distribution Functions

An integral portion of the calculations are the distribution functions. Four functions were utilized; the first (FUN 1) for verification of the program against results obtained by Carrier, *et al.*, for their "STRATUS I" cloud (the closest distribution to our other functions in relative shape, concentration, etc.).[7]

---

[7] L. W. Carrier, G. A. Cato, and K. J. von Essen. "The Backscattering and Extinction of Visible and Infrared Radiation by Selected Major Cloud Models." *Applied Optics 6:7*, 1209 (July, 1967).

The last three functions represent probable distributions of particles in a tornado funnel (which has not contacted the ground). The functions are plotted in Figures 2 through 5 and the associated constants for the distribution function, $n(r) = ar^{\alpha}\exp[-br^{\gamma}]$ are listed in Table 4.

Figure 2 contains two plots, one of the original distribution used by CARRIER, *et al.* and the other the distribution function we used to approximate the original. The results obtained, as the data indicates, are very close to the values obtained originally for all values of wavelength used in this study. Figures 3 and 5 represent the probable maximum and minimum concentrations, respectively, of the expected distributions. Figure 4 represents a median concentration. The concentration, mode radii, and relative dispersion are indicated on each of the figures.

Program Verification

During the initial development of the program, the fundamental Mie parameters defined earlier and described by Equations (2-5) through (2-8) were rigorously checked against published results for the 10 μm range using an index of refraction of $m = 1.212\text{-}i0.0601$.[8,9,10] The values computed matched the values published by Deirmendjian to the accuracy quoted and agreed with those of Gumprecht and Sliepcevich. For the wavelengths of 0.5 μm

---

[8]D. Deirmendjian. *Electromagnetic Scattering*, p. 30.

[9]D. Deirmendjian. *Tables of Mie Scattering Cross Sections and Amplitudes.* Report prepared for United States Air Force Project Rand, #R-407-PR, January, 1963. Santa Monica, CA: Rand Corporation, 1963.

[10]R. O. Gumprecht and C. M. Sliepcevish. *Light-Scattering Functions for Spherical Particles.* Willow Run Research Center: University of Michigan Press, 1951.

Table 4. Distribution Function Constants

Program Name	Mode Radius (μm)	a	b	α	γ
FUN 1	3.5	23.480232	.42341	3	1
FUN 2	5	1.0	0.1	5	2
FUN 3	10	7.81248×10^{-3}	0.025	5	2
FUN 4	15	1.1098×10^{-7}	7.901×10^{-4}	8	3

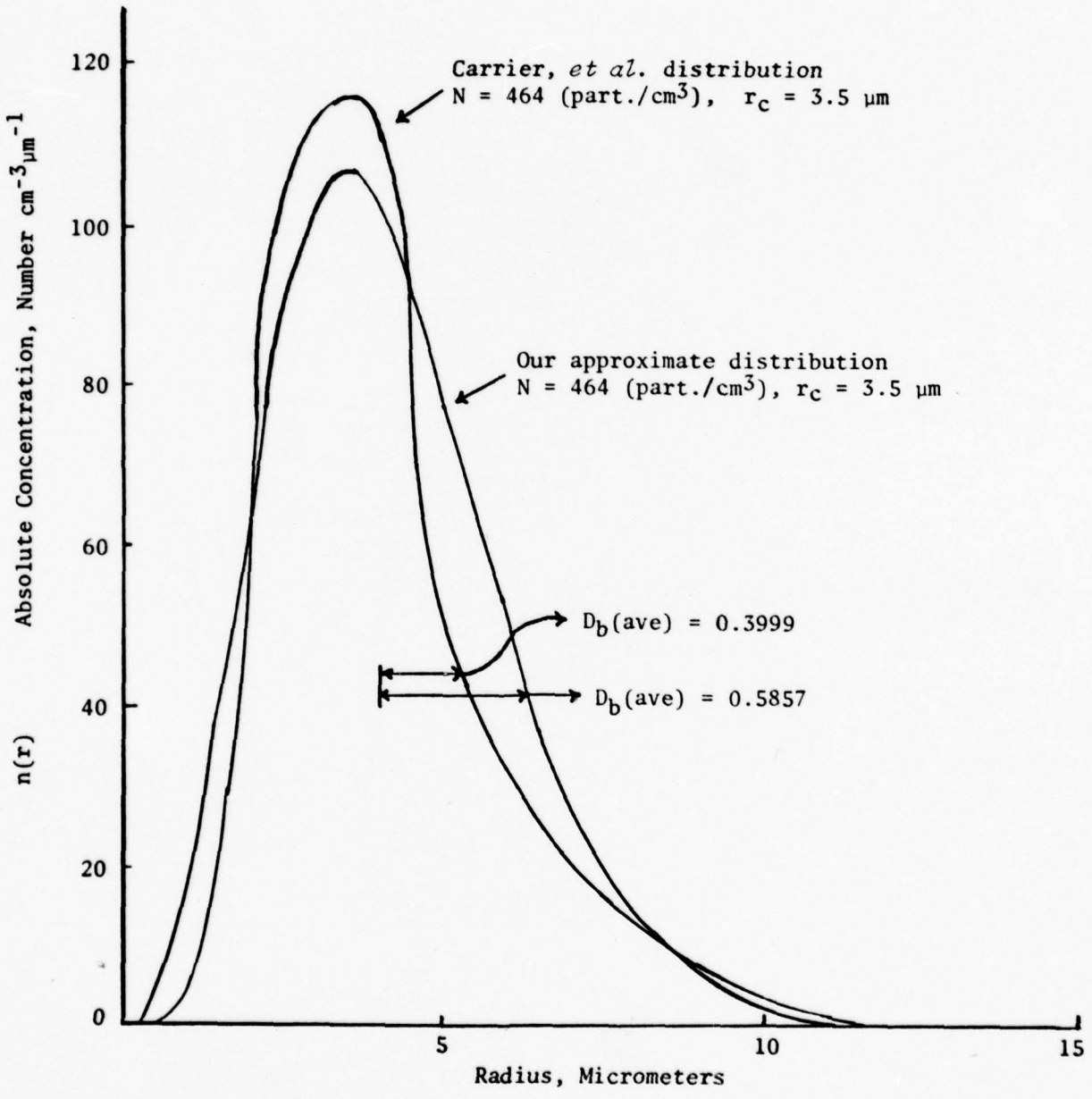

Figure 2. Comparison of test distribution #1 and the stratus I cloud distribution of Carrier, *et al.*

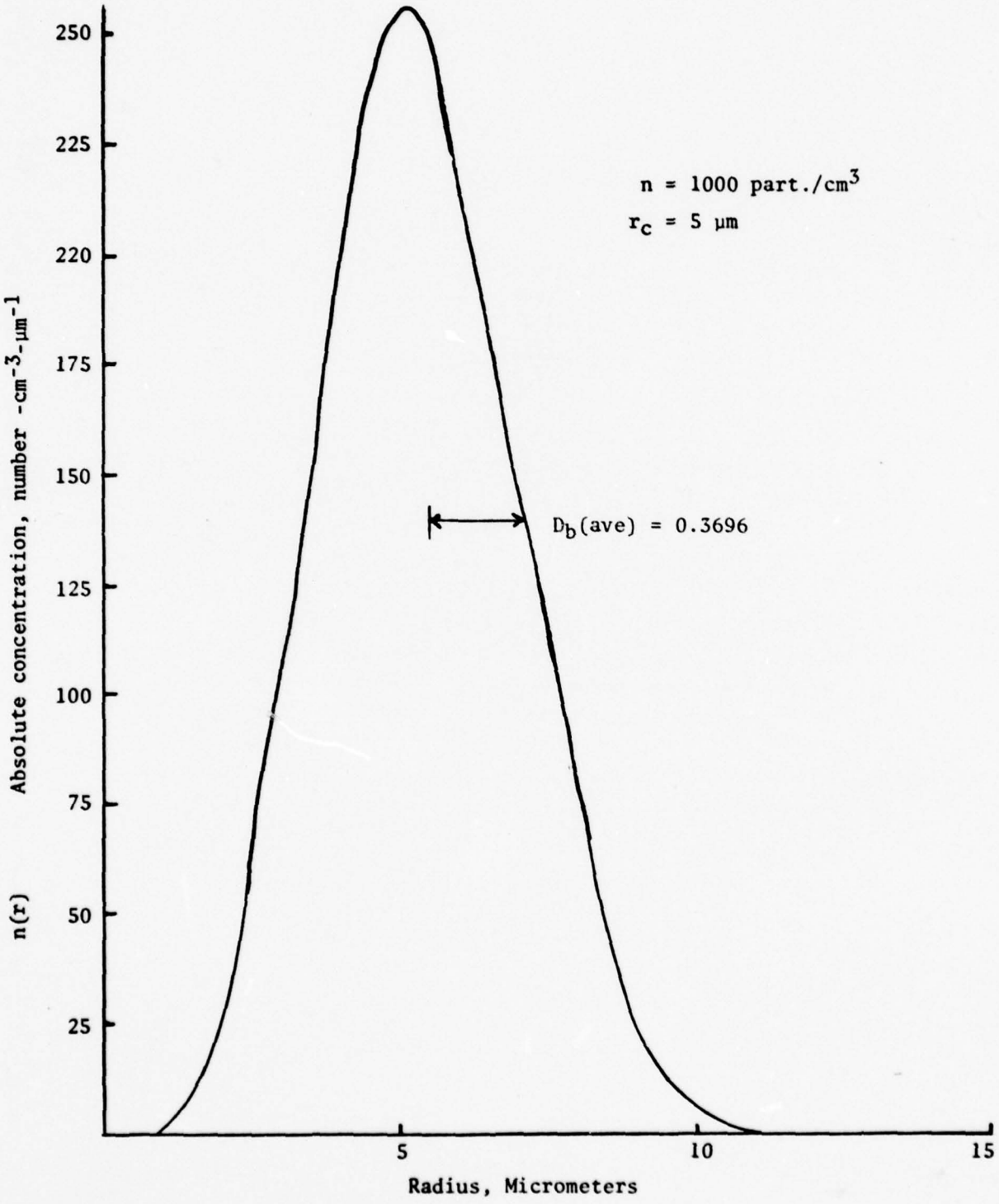

Figure 3. First probable funnel cloud, distribution #2

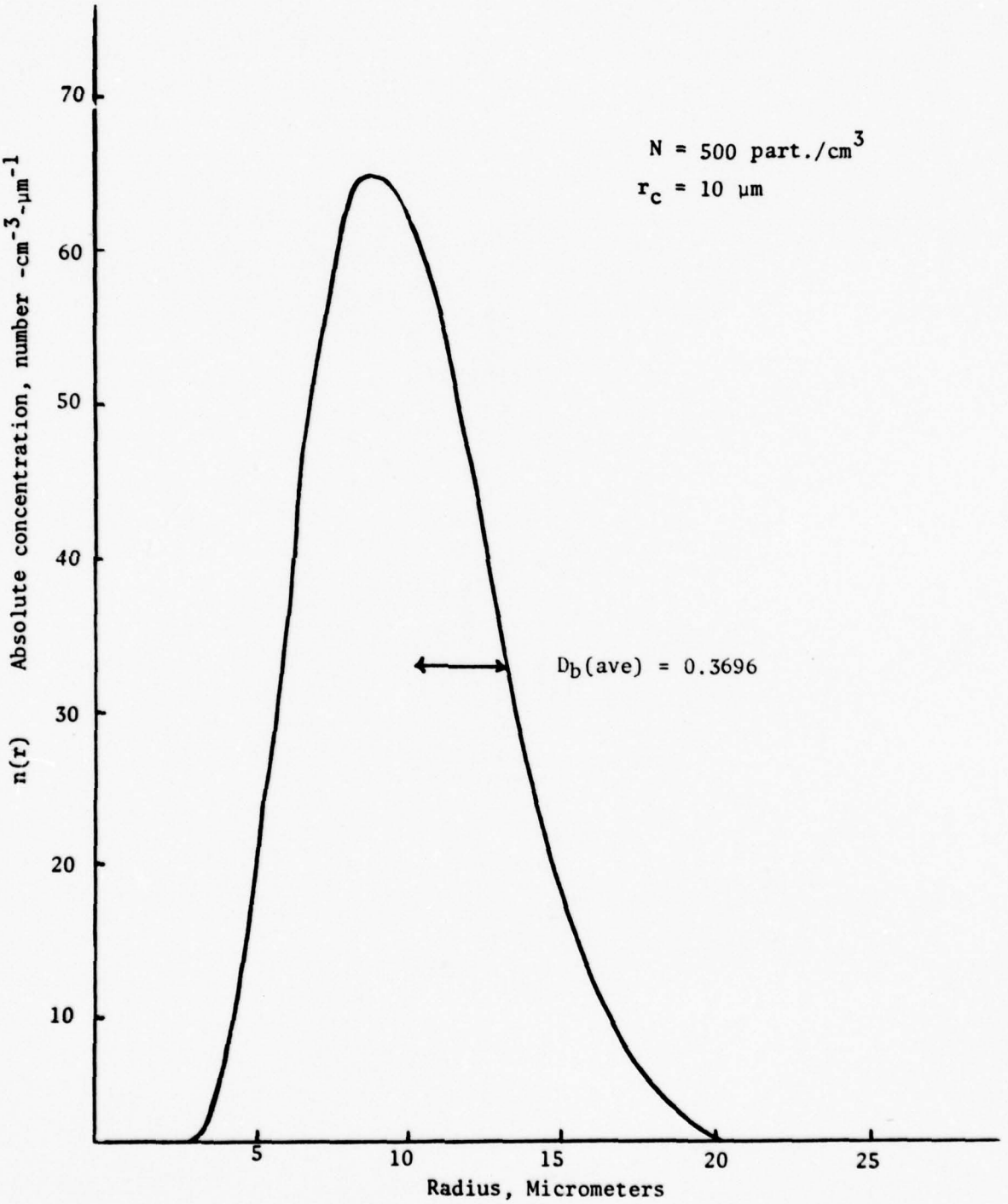

Figure 4. Second probable funnel cloud, distribution #3.

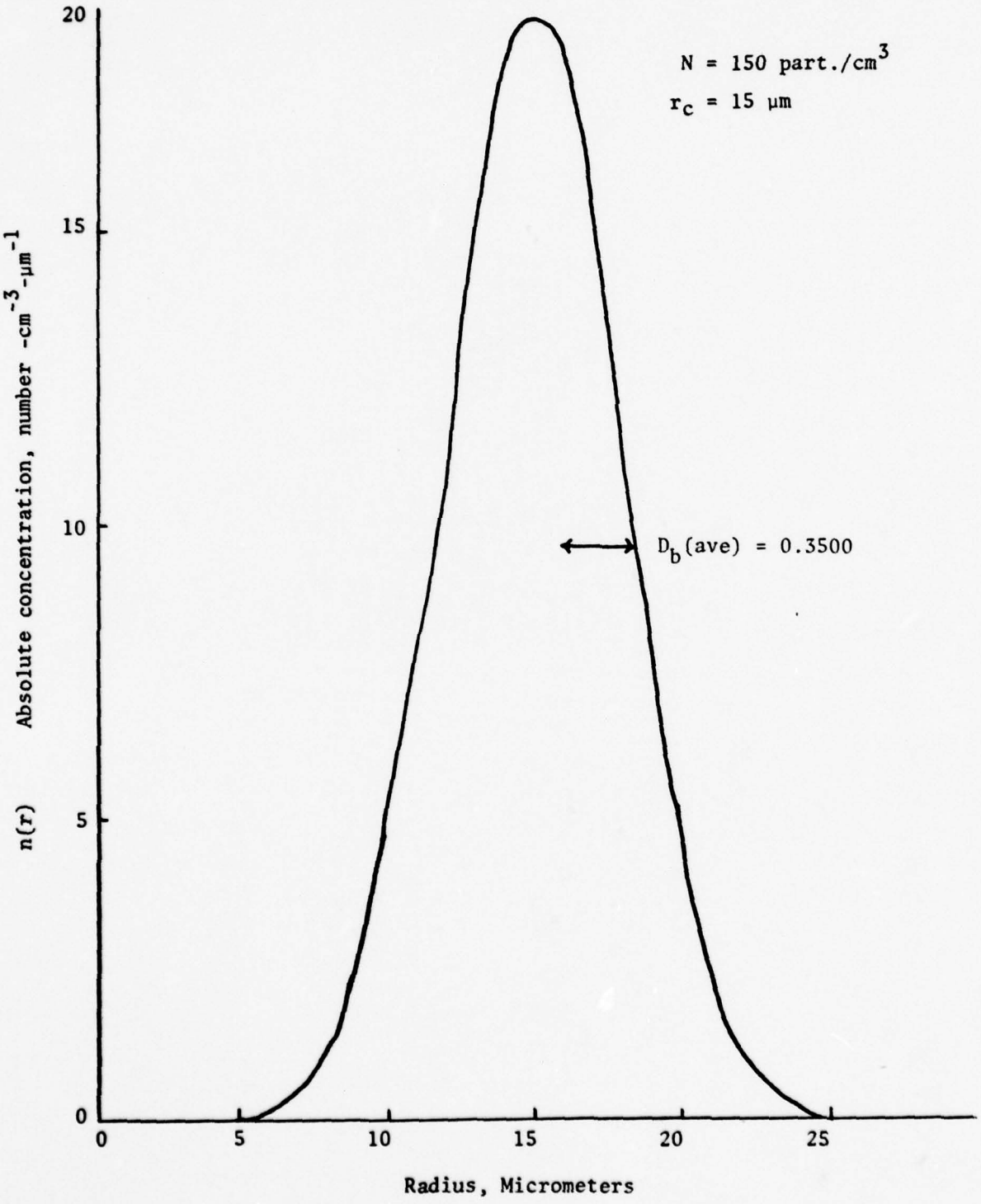

Figure 4. Second probable funnel cloud, distribution #3.

and 1.06 μm with indices of refraction of 1.34 and 1.33 respectively, the computed parameters were printed out at intervals to preclude volumes of numbers. In all cases, the values printed correspond to the published results of Gumprecht and Sliepcevich and matched the values computed from the exact Mie theory as cited by Houghton and Chalker.[11] Published results for index of refraction $m = 1.353\text{-}i0.0059 (\lambda = 4.0\ \mu m)$ were not available for comparison, however, the computed results did correspond quite well in degree of magnitude and inflection with the values published for $m = 1.33$.[12,13]

The values obtained for the extinction and backscatter coefficients were checked by inserting a test distribution which approximated the "Stratus I" cloud of Carrier, *et al.*, (See Figure 2).[14] The values obtained are listed in Table 5 along with the values obtained by Carrier, *et al.*, and the percentage difference computed using the latter values as the standard. The differences in β_{ext} are caused by the narrower relative dispersion at the median of the spectrum of Carrier, which tends to increase β_{ext}.

---

[11] H. G. Houghton and W. R. Chalker. "The Scattering Cross Section of Water Drops in Air for Visible Light," *Journal of the Optical Society of America 39:11*, 955 (November, 1949).

[12] Grumprecht and Sliepcevich, *Light-Scattering Functions*, p. 4.

[13] Houghton and Chalker, "Scattering Cross Section" pp. 955-957.

[14] Carrier, "Backscattering and Extinction" p. 1212.

Table 5. Comparison of Extinction and Scattering Properties for the Test Distribution.

Wavelength (Micrometers)		Computed Values	Carrier, *et al.*[7]	Per Cent Difference
10.6	β_{ext}	3.92×10^{-2} m^{-1}	4.28×10^{-2} m^{-1}	-8.4
	$\beta(\pi)$	6.41×10^{-5} m^{-1} sr^{-1}	7.42×10^{-5} m^{-1} sr^{-1}	-13.6
4.0	β_{ext}	8.46×10^{-2} m^{-1}	9.01×10^{-2} m^{-1}	-6.1
	$\beta(\pi)$	1.25×10^{-3} m^{-1} sr^{-1}	1.47×10^{-3} m^{-1} sr^{-1}	-15.0
1.06	β_{ext}	6.80×10^{-2} m^{-1}	6.97×10^{-2} m^{-1}	-2.4
	$\beta(\pi)$	3.59×10^{-3} m^{-1} sr^{-1}	3.08×10^{-3} m^{-1} sr^{-1}	+16.6
0.5	β_{ext}	6.54×10^{-2} m^{-1}	6.69×10^{-2} m^{-1}	-2.2
	$\beta(\pi)$	3.49×10^{-3} $m^{-1}sr^{-1}$	$3.13\times10^{-3}m^{-1}sr^{-1}$	+11.5

The positive increase in the values of $\beta(\pi)$ at 1.06 μm and 0.5 μm is predicted by the analysis of Carrier, and is presumably due to a combination of broader spectrum and larger particle concentration in the range of 4.5 to 8 μm of the approximate distribution.[15] However, this same condition apparently decreases $\beta(\pi)$ for the larger wavelengths.

The first test distribution (Figure 3) has a mode radius that is close to some cloud models; however, it differs in the concentration of particles. Comparing the results for the extinction coefficient with Deirmendjian's cloud model,[16] the computed values were slightly higher (within 25%) for the comparable wavelengths of 0.45 μm, 1.61 μm, 3.90 μm, and 10 μm. The higher values are to be expected since the mode radius of Deirmendjian's model is lower (4 μm) than that of the test distribution (5 μm).

Comparing the results to the "alto-stratus" cloud of Carrier, *et al.*, which is closer in mode radius (4.5 μm), the computed values of β_{ext} are lower by approximately 17 per cent for λ = .488 μm, 1.06 μm and 4.0 μm and 30 per cent for λ = 10.6 μm, which may be attributed to the large concentration of particles in the 10-13 μm range in the "alto-stratus" cloud. The computed values for $\beta(\pi)$ are again low by 42 per cent, 5 per cent, 54 per cent, and 28 per cent for λ = .488 μm, 1.06 μm, 4.0 μm, and 10.6 μm respectively. With the exception of the values for 0.5 μm and 4.0 μm, these lower values may similarly be attributed to the broadened concentration

---

[15] *Ibid.*, p. 1209.

[16] Deirmendjian, *Scattering and Polarization*, p. 9.

above 10 μm in the alto-stratus distribution. The reason for the low value at these wavelengths is not immediately evident; however, Carrier suggests that broadening can decrease $\beta(\pi)$ by factors in the 50 per cent range and so these values are not considered invalid.[17]

[17]Carrier, *Backscattering and Extinction*, p. 1212.

CHAPTER IV

ANALYSIS OF DATA

The data produced by the computer program is tabulated in Appendix D. Tables 6 and 7 contain listings of the extinction- and backscattering-coefficients for the wavelengths, step size, and distributions shown.

To determine the optimum operating conditions we consider the wavelength and the length of the scattering volume, ignoring for the moment the practical side of what is currently available in the way of transmitter power and special requirements of sensitive detectors (such as low temperature operation). Our aim is to maximize the ratio of intensity received to intensity transmitted.

The wavelengths utilized were selected with an eye towards the transmission "windows" that occur in the infrared region of the spectrum. As indicated by Equation (1-6), four wavelength dependent factors affect the intensity ratio: (1) the field of view, (2) the extinction factor within the turbulence itself, (3) the amount of radiation scattered back at the receiver, and (4) the transmissivity of the intervening medium. The first three factors have been included in the computer program computations with the results plotted for individual wavelengths of the receiver intensity, normalized to a transmitter spectral irradiance of 1 watt/m^2 versus the distribution

Table 6. Extinction Coefficients of the Various Distributions, β_{ext} (meters)$^{-1}$.

λ(Δr) (micrometers)	Distribution			
	#1	#2	#3	#4
10.6 (.253)	3.91808-02 (0.170)*	1.30680-01 (0.568)	4.73336-01 (2.056)	3.00532-01 (1.305)
10.6 (.506)	3.91785-02 (0.170)	1.30681-01 (0.568)	4.73320-01 (2.056)	3.00427-01 (1.305)
4.0 (.255)	8.46463-02 (0.368)	2.40473-01 (1.044)	4.32330-01 (1.878)	2.46862-01 (1.072)
4.0 (.477)	8.47518-02 (0.368)	2.41875-01 (1.050)	4.34119-01 (1.885)	2.47657-01 (1.075)
1.06 (.253)	6.80013-02 (0.295)	2.06574-01 (0.897)	3.99796-01 (1.736)	2.31788-01 (1.007)
0.50 (.251)	6.53955-02 (0.284)	1.99431-01 (0.866)	3.90475-01 (1.696)	2.27353-01 (0.987)

*Figures in parentheses indicate loss in db/meter.

Table 7. Backscatter Coefficients of the Various Distributions, $\beta(\pi)$ $(meter)^{-1}(steradian)^{-1}$.

$\lambda(\Delta r)$ (micrometers)	Distribution			
	#1	#2	#3	#4
10.6 (.253)	6.40959-05	1.99547-04	2.1000-04	1.00082-04
10.6 (.506)	6.40957-05	1.99548-04	2.09992-04	1.00032-04
4.0 (.255)	1.24974-03	3.87723-03	1.18300-02	3.37952-03
4.0 (.477)	1.14929-03	3.63343-03	1.23361-02	3.54947-03
1.06 (.253)	3.59016-03	1.05844-02	2.31075-02	1.21906-02
0.50 (.251)	3.49286-03	8.69341-03	2.49455-02	1.44447-02

functions in Figures 6-9. Figures 10-12 are comparison plots of the normalized receiver intensity for the different wavelengths versus a particular distribution function. When interpreting Figures 6-12, it is important to remember that the spectral irradiance of the pulse is the factor that has been kept constant, which results in the decrease in receiver intensity for the longer lengths of the scattering volume. If the amplitude of the pulse is kept constant and the pulse varied, then the receiver intensity will increase for longer length of the scattering volume. The transmissivity factors for all four wavelengths are computed from Table 2. From the calculations, it is evident that the property of high transmissivity that so enhances the use of the 10.6 μm laser also hinders it in this study as the backscattered radiation is proportionately low. From Figures 10-12 it is clear that the intensity ratio of the 4.0 μm laser is significantly greater than the intensity ratios of either the 10.6 μm, the 1.06 μm, or the 0.5 μm laser except for Distribution #2, which indicates that the intensity ratios of the 10.6 μm line is comparable to that of the 4.0 μm line, especially when the transmissivity of the two are taken into consideration. Furthermore, the extinction of the 0.5 μm line decreases its intensity level to a point that virtually eliminates it from further consideration.

The length of the scattering volume is important since it effectively determines the amount of backscattered radiation produced. Our primary concern is to limit the backscattered radiation to that which is singly scattered (thus eliminating multiply-scattered

velocities) while maximizing the amount of backscattered intensity. Presumably, an unlimited length of the scattering volume would result in the maximum return of unpolarized radiation from all modes of scattering. To determine the point at which second- and higher-order scattering become significant we relate that point to the optical depth, $\tau = \beta_{ext} L$. From the results of Anderson and Browell,[1] it appears that the ratio of second-order backscatter to first-order backscatter is about 10 per cent at $\tau = 0.25$; 28 per cent at a τ of 1.0; and 36 per cent at a τ of 4.0 for a wavelength of 0.9 μm. If we assume similar figures for the wavelengths of 1.06-, 4.0-, and 10.6-μm then a reasonable optical depth would be $\tau = 1.0$. (We note at this point that polarizing our initial radiation will aid in eliminating at least 50 per cent of the multiply-backscattered radiation while not affecting the first-order scattering.) The resultant length of scattering volume for an optical depth of 1.0 are listed in Table 8 for each of the wavelengths and distributions considered.

Distribution #3, corresponding to a concentration of 500 particles/cm and a mode radius of 10 μm, is seen to be considerably lower than the other distributions indicating heavy losses for this distribution as is confirmed by Figures 6-9.

Setting the depth of scattering in accordance with the values in Table 8 will automatically include the maxima of the backscatter curves in Figures 5-10 since the maximum (as computed by setting

---

[1] Anderson and Browell, *First- and Second-Order Backscattering"* p. 1348-1350.

Table 8. Proposed Single Scattering Lengths.*

Wavelengths (micrometers)	Distributions		
	#2	#3	#4
10.6	7.64	2.12	3.32
4.0	4.16	2.32	4.04
1.06	4.88	2.5	4.32
0.50	5.01	2.56	4.39

*Lengths in meters.

the first derivative of the function equal to zero) of the Backscatter function occurs at $\tau=(2\beta_{ext})^{-1}$ which is ½ each value indicated in Table 8. We relate this to pulse length in the following manner; a depth of scattering of four meters would correspond to a pulse length of $4m/3\times10^{8}$ $msec^{-1}$ = $1\ 1/3\times10^{-8}$ sec or about thirteen nanoseconds which has been achieved in lasers of wavelength 1.06 μm and 4.0 μm,[2] and can theoretically be achieved by mode locking or modulating by absorbable dyes in a 10.6 μm laser.

In Chapter II we computed values for the transmissivity of the atmosphere (the intervening medium) and signal power for the various wavelengths. Using a median value of transmissivity, signal power corresponding to an SNR = 10, and the results of this chapter, we have compiled in Table 9 representative figures for the required power of a laser employing a 6-inch (15.24 cm) lens (diffraction-limited detector), operating over a 10 km path length. The figures were computed by the following formula: P_T = Req'd Output Powers = $\frac{A_T P_S}{\tau_A^2(\text{Scatter Ratio})}$ (watts) where A_T is area of the lens, P_S is the required signal power, τ_A is the transmissivity of the atmosphere and scatter ratio is the level of ackscattered radiation computed for a spectral irradiance, $H(\lambda)$, of 1 watt/meter^2 over the scattering lengths given in Table 8. These values clearly show that the primary wavelenths to consider are 10.6 μm and 1.06 μm with the former having a slight edge in average power required.

---

[2] A. Kestenbaum. "Laser Processing Fundamentals." *Lasers in Industry*. ed. S. S. Charschan. New York: Van Nostrand Reinhold Co., 1972.

Table 9. Power Required for Operation of the System.*

Wavelength (micrometers)	10.6	4.0	1.06	0.50
Transmissivity (τ_A^2) (dimensionless)	4.7×10^{-5}	6.2×10^{-8}	4.4×10^{-3}	8.9×10^{-5}
Required Signal Power (watts)	1.41×10^{-11}	9.94×10^{-11}	1.41×10^{-9}	6.36×10^{-9}
Scatter Ratio (dimensionless)				
Distribution #2	1.30×10^{-12}	1.85×10^{-12}	4.05×10^{-13}	8.1×10^{-14}
Distribution #3	3.6×10^{-13}	3.5×10^{-12}	4.8×10^{-13}	1.18×10^{-13}
Distribution #4	2.8×10^{-13}	1.6×10^{-12}	4.4×10^{-13}	1.18×10^{-13}
Required Output Power (watts)				
Distribution #2	4.21×10^{3}	1.58×10^{7}	1.44×10^{4}	1.61×10^{6}
Distribution #3	1.52×10^{4}	8.36×10^{6}	1.22×10^{4}	1.1×10^{7}
Distribution #4	1.95×10^{4}	1.83×10^{7}	1.33×10^{4}	1.1×10^{7}
Average	1.3×10^{4}	1.42×10^{7}	1.33×10^{4}	7.87×10^{6}

*Average power.

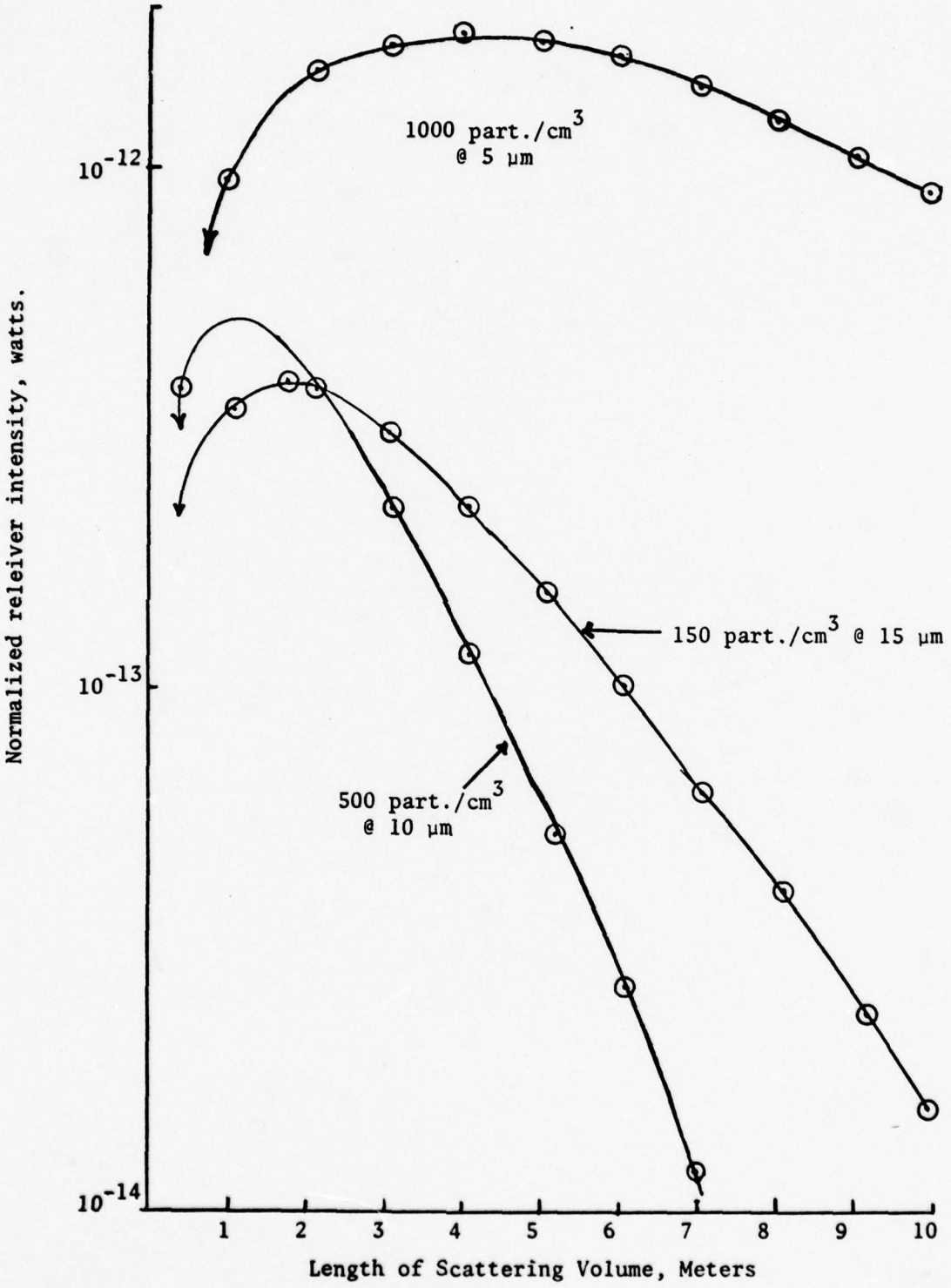

Figure 6. Plot of normalized receiver intensity vs. length of scattering volume for all funnel cloud distributions at a wavelength of 10.6 μm.

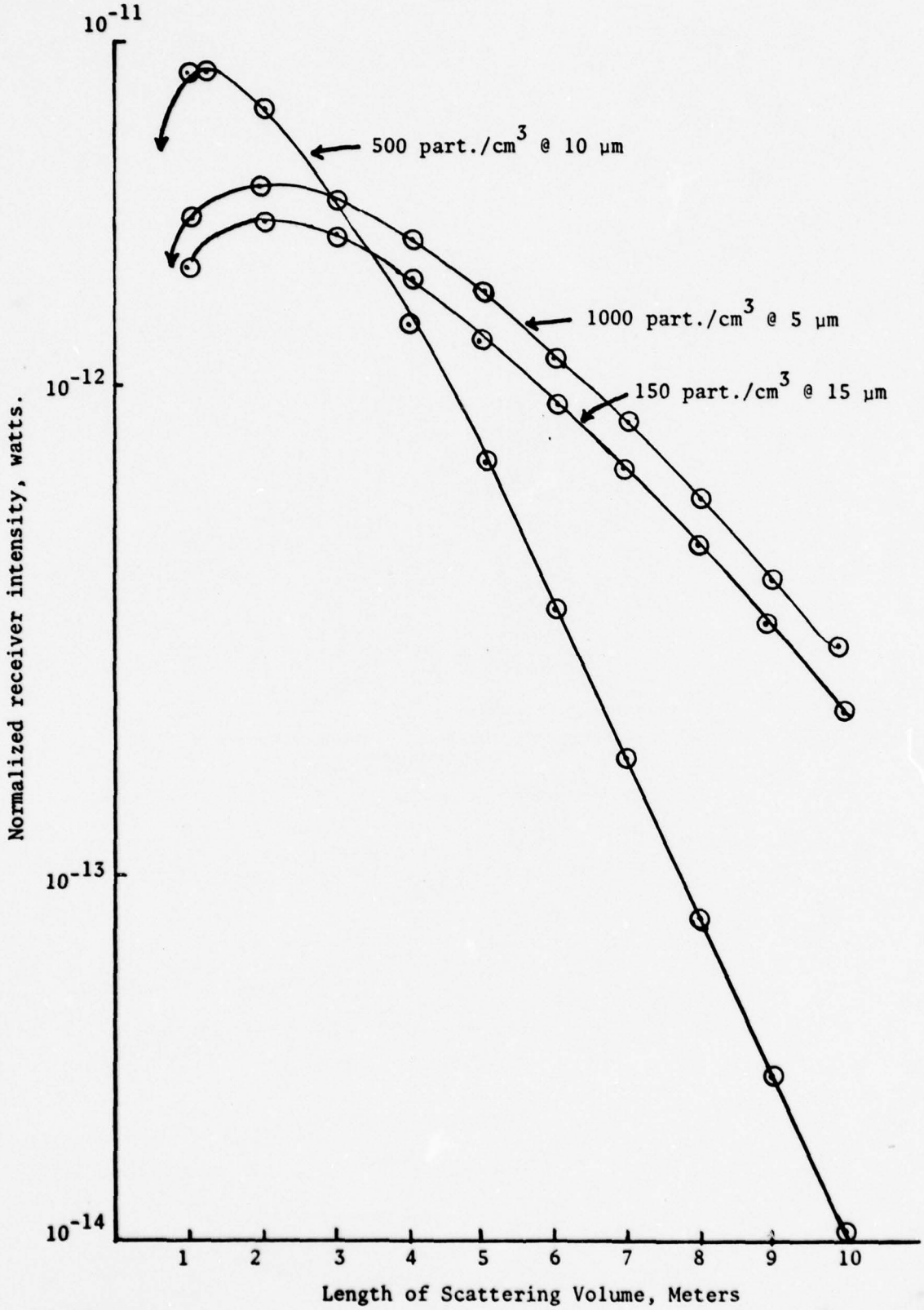

Figure 7. Plot of normalized receiver intensity vs. length of scattering volume for all funnel cloud distributions at a wavelength of 4.0μm.

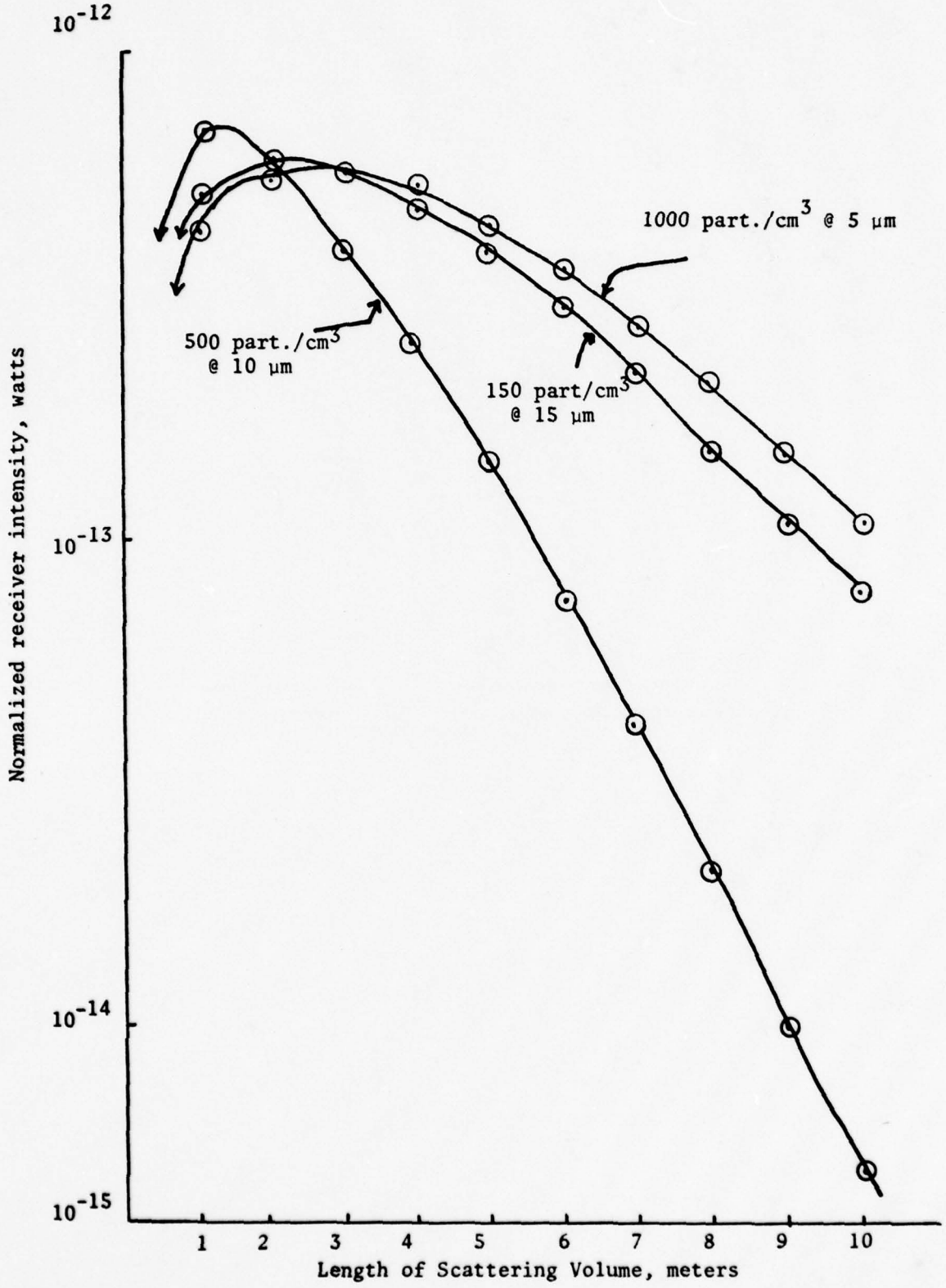

Figure 8. Plot of normalized receiver intensity vs. length of scattering volume for all funnel cloud distributions at wavelength of 1.06 μm

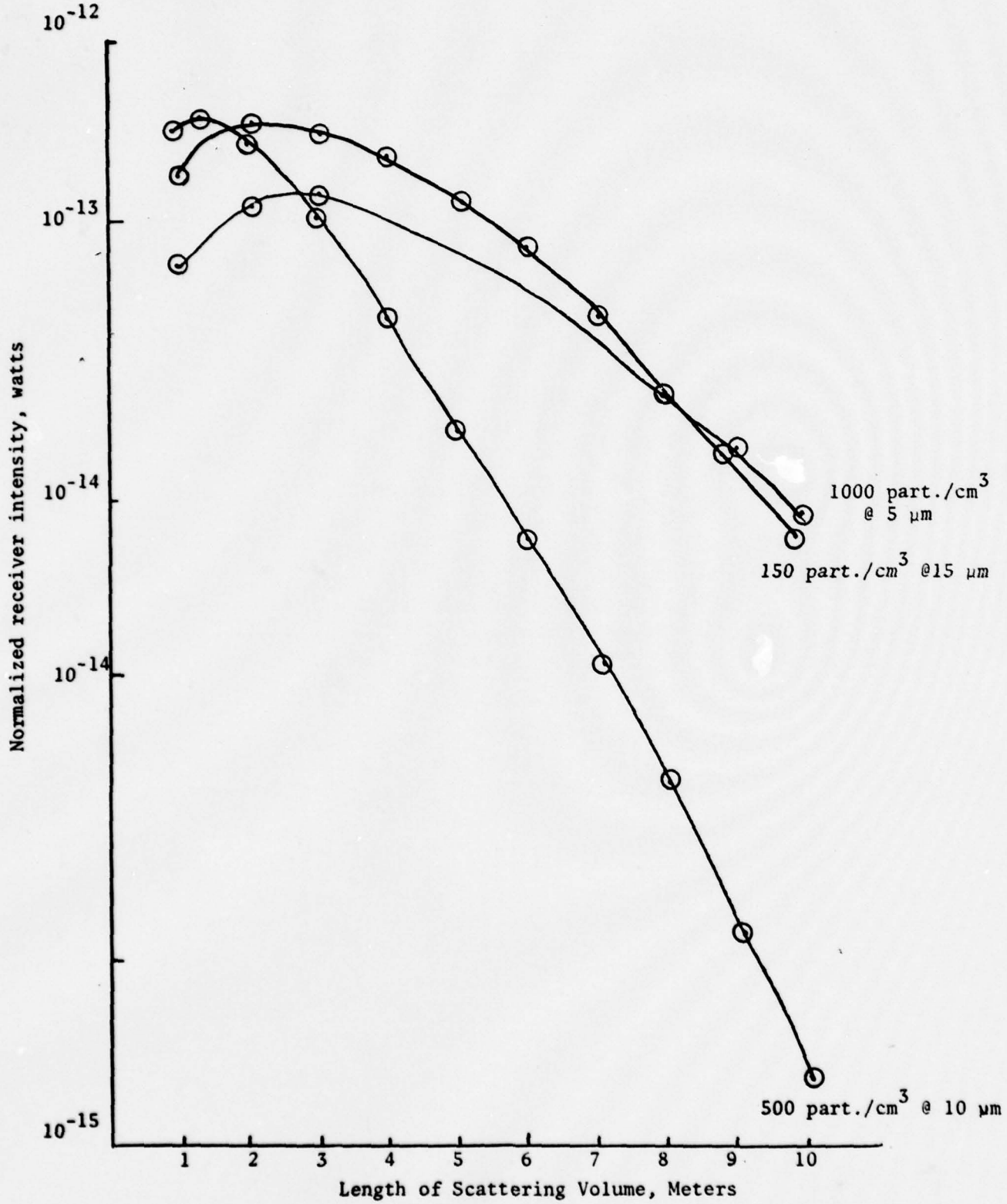

Figure 9. Plot of normalized receiver intensity vs. length of scattering volume for all funnel cloud distributions at a wavelenght of 0.5 μm

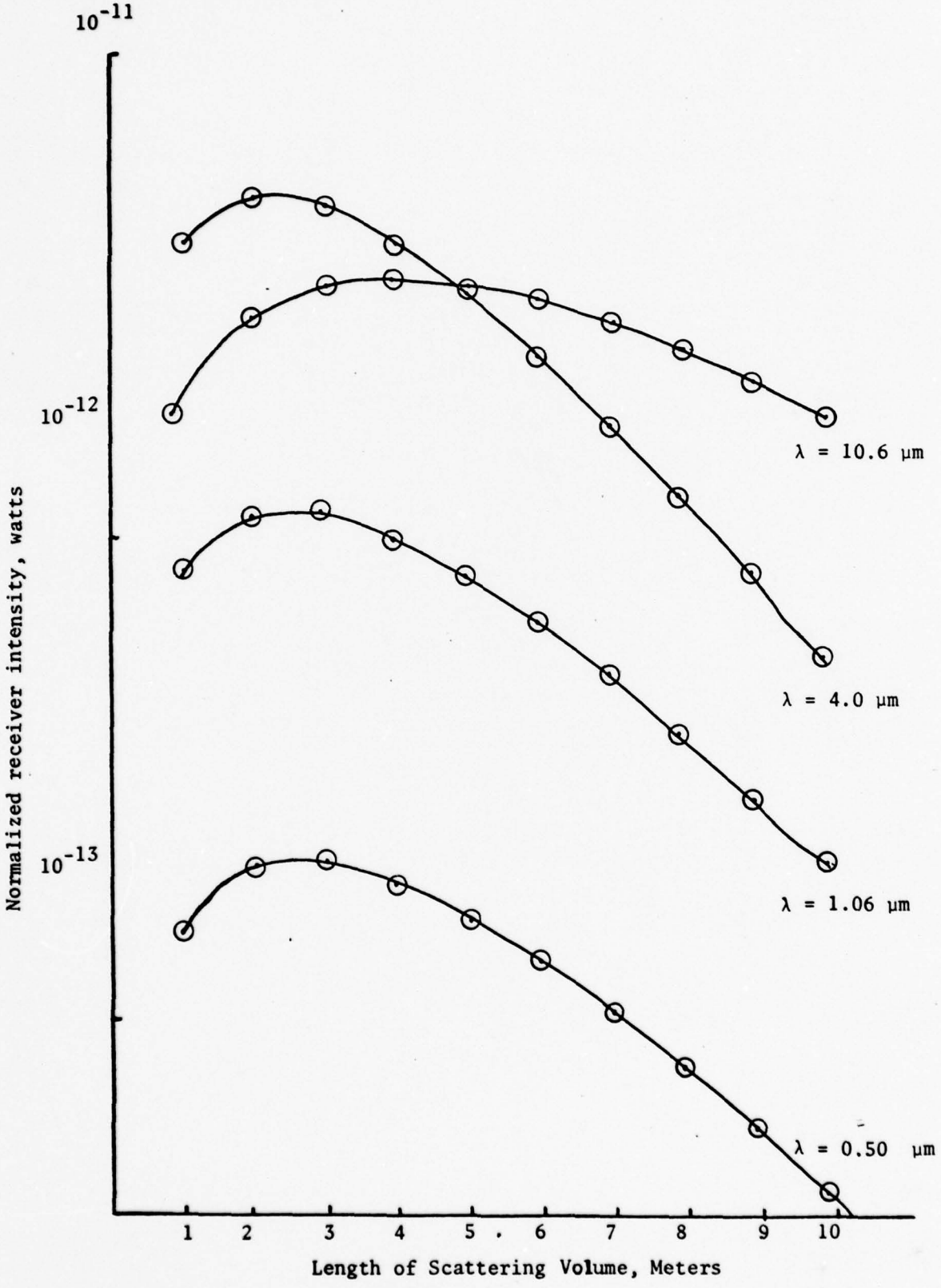

Figure 10. Plot of normalized receiver intensity vs. length of scattering volume at all wavelengths for distribution #3.

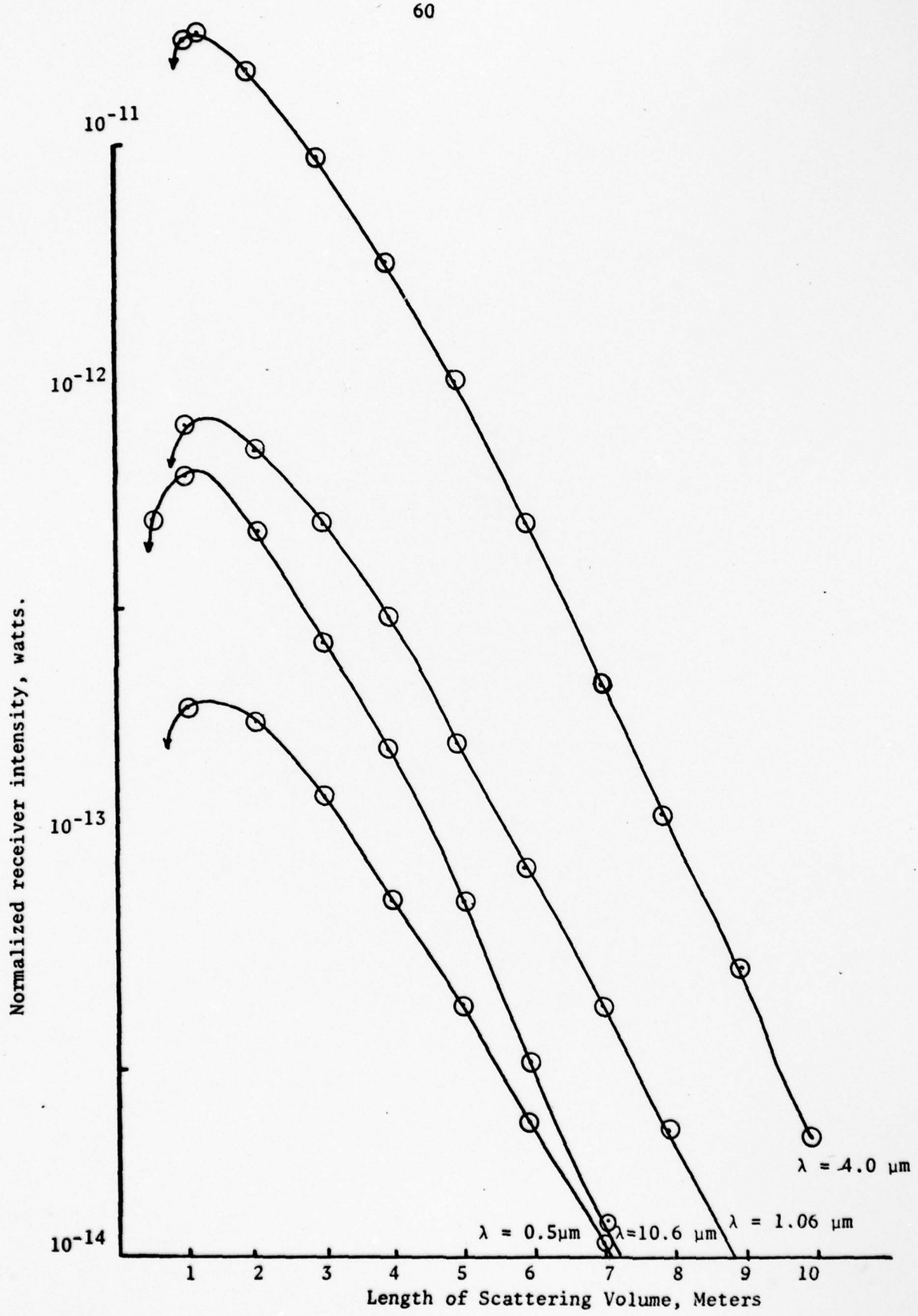

Figure 11. Plot of normalized receiver intensity vs. length of scattering volume at all wavelengths for distribution #4.

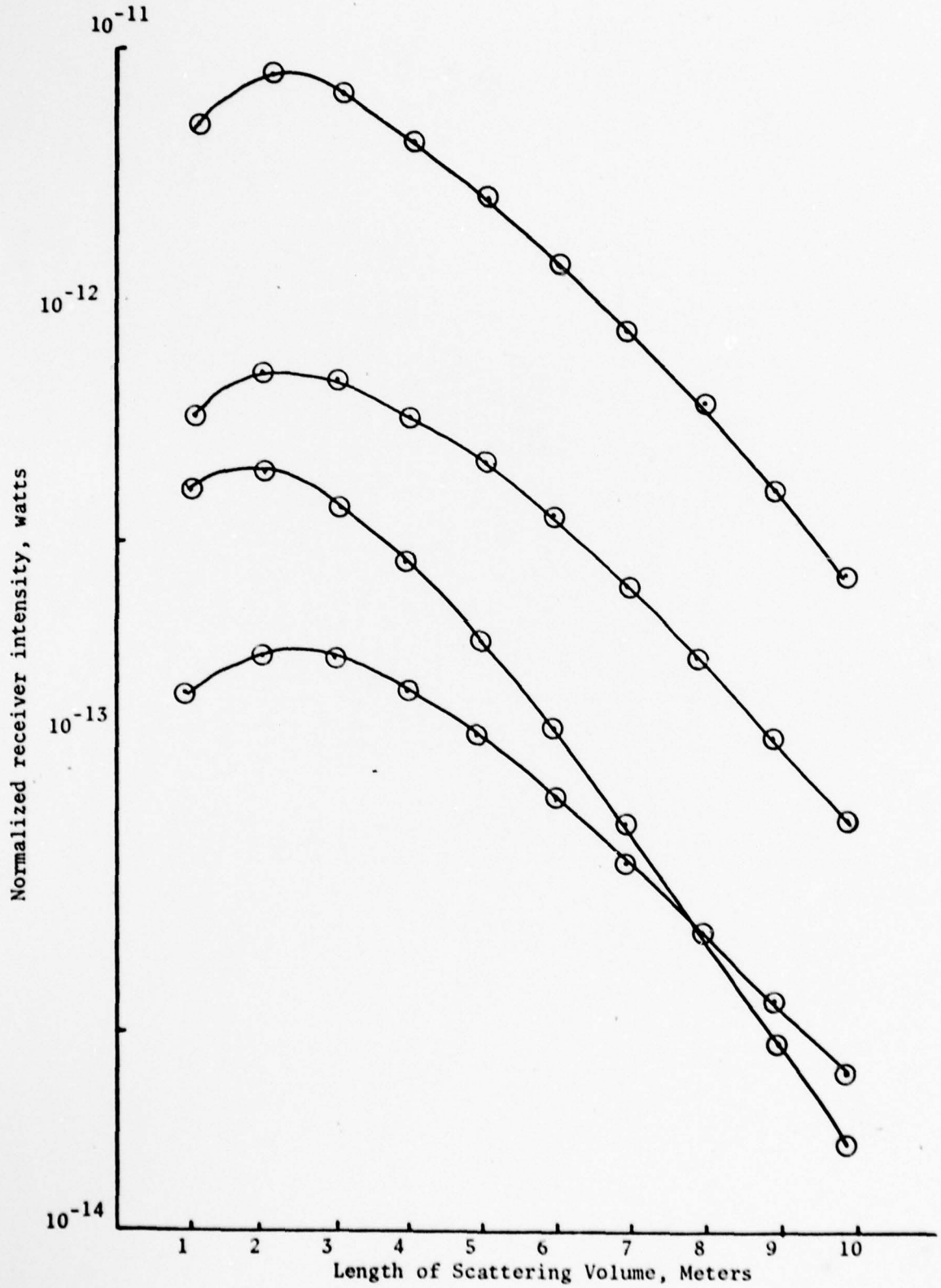

Figure 12. Normalized receiver intensity vs. length of scattering volume at all wavelengths for distribution #4.

CHAPTER V

SUMMARY, CONCLUSIONS, AND RECOMMENDATION

The purpose of this paper was to determine the feasibility of utilizing pulsed lasers to determine the velocity structure of the turbulence associated with tornadoes. To this end, a computer program was developed using Mie parameters to obtain the extinction and backscatter properties associated with the particles presumed to be distributed within the tornado. The program was then used to analyze three possible distributions of particles with four different wavelengths. The data obtained were (1) the extinction and backscatter coefficients of the various wavelengths for those distributions, and (2) the associated backscatter intensity ratios (for the various distributions and wavelengths) evaluated per length of scattering volume for a specified, diffraction limited field-of-view and a specified scattering area. In addition, the computer program will output the Mie parameters for any desired value of the size parameter, $x = 2\pi r/\lambda$, and it is adaptable to other continuous distributions or a combination of continuous distributions.

It was determined that a SNR = 10 could be achieved using pulse widths of the order of 10-20 nanoseconds and output powers of the order of 10 kilowatts. To achieve these figures, we used a 10 km, clear-air approach medium and an aligned, diffraction-limited,

heterodyne receiver with a 15.24 cm (diameter) lens.

Of the wavelengths considered, it was determined that 10.6 μm and 1.06 μm are the most conducive to this type of use while 0.5 μm will be severely handicapped by the funnel cloud distributions and 4.0 μm is a victim of the intervening medium (specifically, molecular absorption).

Three distributions (designed as limiting distributions), with particle radii on the order of 1-25 μm, were utilized to represent probable conditions found in tornado funnel clouds. The results obtained were, in general, applicable to all three distributions.

Conclusions

From the data obtained in this study, it appears that a pulsed laser operating in the near infrared has the capability to deliver sufficient power to project electromagnetic radiation through the atmosphere to a range of up to 10 km, scatter that radiation from a turbulent distribution of particles, to return and to provide a measureable signal to a coaxially mounted detector. Table 10 indicates the power required for various ranges up to 10 km.

The velocity spectra obtained as a result of implementing such a system is, of itself, limited in the sense that a velocity so obtained is the total instantaneous velocity of a particle in the direction of the observer at the time of scattering. There is no discrimination between the various translational and rotational components of this velocity. Further, there is no indication of

Table 10. Minimum Power Requirements at 10.6 μm for the Various Distributions versus Range (Power in Watts).*

Distribution	Range (kilometers)				
	1	3	5	8	10
#2	0.54	3.93	28.9	573.4	4.2×10^3
#3	1.94	14.2	104.2	2.07×10^3	15.2×10^3
#4	2.49	18.3	134.0	2.66×10^3	19.5×10^3
Average	1.66	12.1	89.0	1.77×10^3	13.0×10^3

*Average power.

movement in the direction vertically perpendicular to the direction of propagation. However, it is anticipated that one may obtain some of this information by moving the laser beam in a coordinated manner both horizontally and vertically and thus obtain a mapping of the instantaneous velocities of the tornado. Comparison between the velocities obtained on one side of the tornado and its horizontal counterpart on the other side of the tornado would provide some indication of the relationship between the rotational and translational velocities since the two spectra then represent approaching and receding velocities.

The data obtained, though limited to the distributions cited, is considered a good indication of the limiting conditions likely to be found in a funnel cloud. There are other conditions that are natural extensions of the work initiated here and resulting analysis of these conditions may be conducted utilizing the existing computer program. Examples include the investigation of distributions that would result from contact with the ground such as the distribution of prairie dust or that of a plowed field. Also, investigation of the distribution of rain should be analyzed to determine to what extent the signal is further degraded. Probable distributions of rain have been suggested by the work of Rensch and Long.[1] It is anticipated that rain could conceivably eliminate the possibility of sufficient backscatter being received by the detector and

---

[1]Rensch and Long, *Comparative Studies*, pp. 1566-67.

the need to select an optimum direction from which one would direct the laser beam becomes apparent.

(cont. from p. 1)

Recommendation

Laser technology has progressed to the point that velocity discrimination on the order of 1 m/sec is achievable outside the laboratory. Furthermore, detectors are available (at the cited wavelengths) with sensitivities of the order required to process the returned signal. However, it is recommended that a system containing the required components including the ancillary equipment be constructed and tested to verify the results obtained in this study.

APPENDIX A

ADAPTATION OF MIE PARAMETERS TO COMPUTER ITERATIONS

The objective is to obtain the expressions (2-5) through (2-8) in the text. Therefore we must express a_n, b_n, π_n, τ_n, and A_n in iterative form and determine the initial values of those iterations. These are,

$$a_n = \frac{(\frac{A_n}{m} + \frac{n}{x})R_e\{W_n\} - R_e\{W_{n-1}\}}{(\frac{A_n}{m} + \frac{n}{x})W_n - W_{n-1}}$$

$$b_n = \frac{(A_n m + \frac{n}{x})Re\{W_n\} - R_e\{W_{n-1}\}}{(A_n m + \frac{n}{x})W_n - W_{n-1}}$$

$$W_n = \frac{2n-1}{x} W_{n-1} - W_{n-2}$$

$$W_o = \sin x + i\cos x$$

$$W_{-1} = \cos x - i\sin x$$

$$A_n = -\frac{n}{mx} + \frac{1}{\frac{n}{mx} - A_{n-1}}$$

$$A_o = CTN(mx) = \frac{\cos mx}{\sin mx}$$

Since mx is a complex function, we expressed this value in the

following form: with $m = r + ik$

$$A_o = \frac{\cos rx \sin rx - i \sinh kx \cosh kx}{\sin^2 rx \cosh^2 kx + \cos^2 rx \sinh^2 kx}$$

instead of the value used by Deimendjian in the cited reference.

The values for the angle dependent function π_n and τ_n were computed for $\theta = \pi$ prior to inserting them into the program. Their values are:

$$-\pi_n(\pi) = \tau_n(\pi) = (-1)^n \frac{n(n+1)}{2} \quad .[1]$$

---

[1]Deirmendjian and Clasen, *Light Scattering*, pp. 35-36.

APPENDIX B. FLOWCHART OF COMPUTER PROGRAM

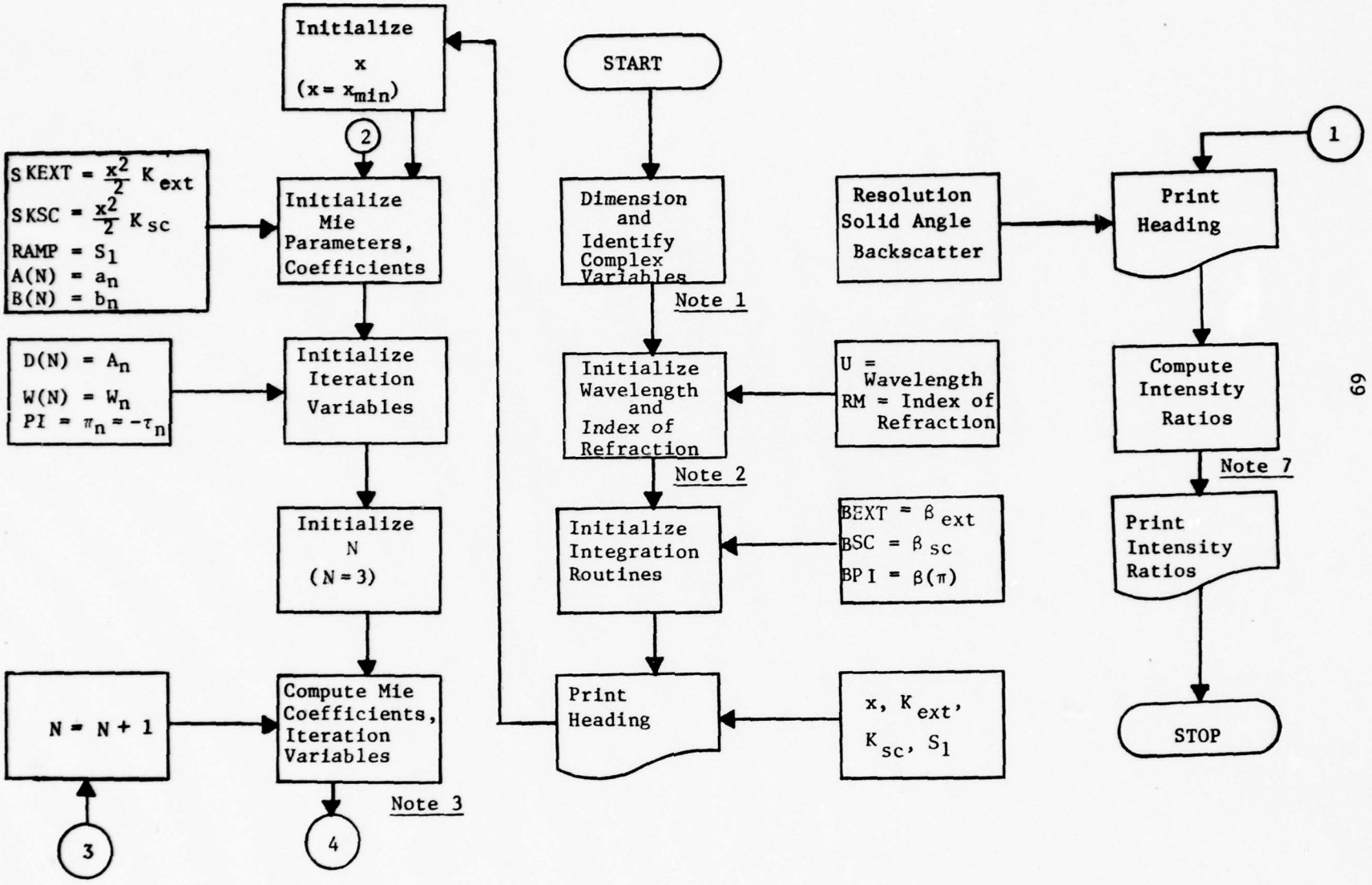

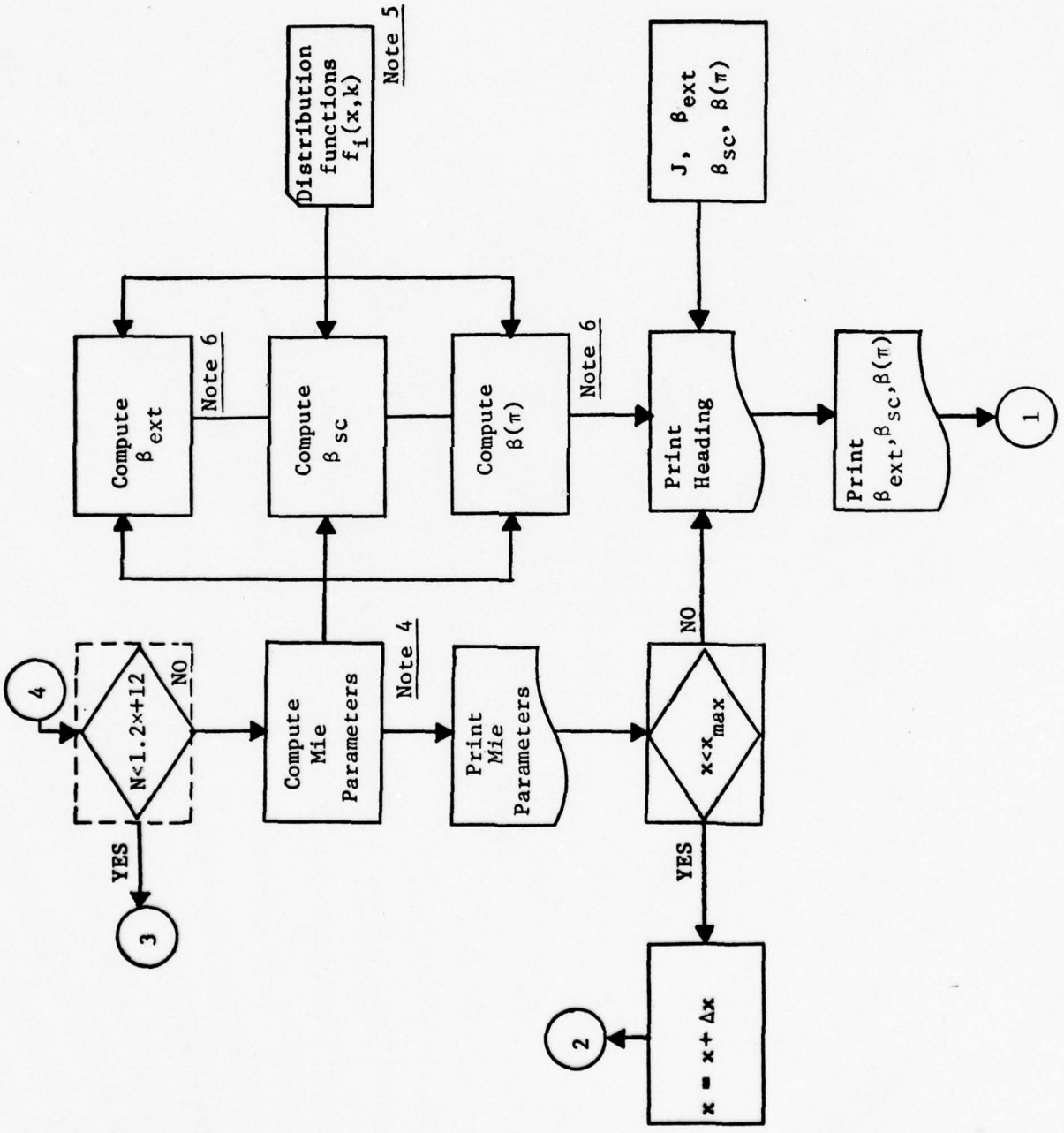
Distribution functions $f_1(x,k)$
Note 5
J, β_{ext} β_{sc}, $\beta(\pi)$
Compute β_{ext}
Note 6
Compute β_{sc}
Compute $\beta(\pi)$
Note 6
Print Heading
Print β_{ext}, β_{sc}, $\beta(\pi)$
1
4
N<1.2x+12
NO
YES
3
Compute Mie Parameters
Note 4
Print Mie Parameters
$x<x_{max}$
NO
YES
2
x = x+ Δx

Note 1: Number of array elements, n, is determined by size parameter x. As a minimum, $n = 1.2x + 12$.

Note 2: Wavelength is expressed in micrometers; Index of refraction is a complex function. The values used in this paper are listed in Table B1.

Note 3: The Mie Coefficients and Iteration variables are computed for each x as described in Appendix A.

Note 4: The Mie Parameters are computed for each x as described in the text and repeated for convenience below. Note, however,

$$K_{ext}(x,m) = \frac{2}{x^2} \sum_{n=1}^{1.2x+12} (2n+1)\mathrm{Re}\{a_n+b_n\} \quad \text{(dimensionless)}$$

$$K_{sc}(x,m) = \frac{2}{x^2} \sum_{n=1}^{1.2x+12} (2n+1)(|a_n|^2+|b_n|^2) \quad \text{(dimensionless)}$$

$$S_1(x,m,\pi) = -S_2(x,m,\pi) = \sum_{n=1}^{1.2x+12} \frac{2n+1}{n(n+1)} [a_n\pi_n(\pi)+b_n\tau_n(\pi)] \quad \text{(dimensionless)}$$

that K_{sc} is not required for our study and was not specifically mentioned in the text. It is the normalized Mie scattering cross section and is an added feature of the program. One may wish to use it for various other functions including the calculation of the normalized Mie absorption cross section.

Note 5: The distribution functions are of the form

$$f_i(x,\lambda) = a\left(\frac{\lambda}{2\pi}\right)^{3+\alpha} x^{\alpha} \exp\left\{-b\left(\frac{\lambda}{2\pi}\right)^{\gamma} x^{\gamma}\right\}$$

with the constants a, b, α, γ given in Table 4 , for the various distributions, i.

Note 6: The extinction-, scattering-, and backscatter-coefficients are computed for each distribution by numerical integration. The formulas are given below for convenience. See Note 4 in regards to the scattering coefficient.

$$\beta_{ext}(m,\lambda,x_1,x_2) = \pi\left(\frac{\lambda}{2\pi}\right)^{3+\alpha}(10^{-6})\int_{x_1}^{x_2} a x^{\alpha+2} \exp\left\{-b\left(\frac{\lambda}{2\pi}\right)^{\gamma} x^{\gamma}\right\} K_{ext}\, dx \ m^{-1}$$

$$\beta_{sc}(m,\lambda,x_1,x_2) = \pi\left(\frac{\lambda}{2\pi}\right)^{3+\alpha}(10^{-6})\int_{x_1}^{x_2} a x^{\alpha+2} \exp\left\{-b\left(\frac{\lambda}{2\pi}\right)^{\gamma} x^{\gamma}\right\} K_{sc}\, dx \ m^{-1}$$

$$\beta(\pi,\lambda,m,x_1,x_2) = \left(\frac{\lambda}{2\pi}\right)^{3+\alpha}(10^{-6})\int_{x_1}^{x_2} a x^{\alpha} \exp\left\{-b\left(\frac{\lambda}{2\pi}\right)^{\gamma} x^{\gamma}\right\} |S_1(\pi)|^2 dx \ m^{-1}\text{-}sr^{-1}$$

Note 7: The intensity ratios (BACKSCATTER) are computed for a specific field of view and scattering area (OMEGA) over values of the scattering length (RESOLUTION) of from 1 to 10 meters according to the formula.

$$\frac{\text{RECEIVER INTENSITY}}{H(\lambda)} = AL\Omega\beta(\pi)\exp(-2L\beta_{ext}) \quad \text{(dimensionless)}$$

Note that it does not consider the transmissivity of the intervening medium.

Table B1. Indices of Refraction

Wavelength (Micrometers)	Complex Index of Refraction, RM(=m)
10.60	1.212-i 0.0601
4.00	1.353-i 0.006
1.06	1.33-i 0.000
0.50	1.34-i 0.000

APPENDIX C

COMPUTER RUN

```
$JOB
C       NOTE1:  THE FIRST PORTION OF THIS PROGRAM - THRU LINE 62 - COMPUTES THE
C       MIE PARAMETERS REFERRED TO AS THEEXTINCTION AND SCATTERING EFFICIENCIES.
C       LABELED'EXT' AND'SCT' RESPECTIVELY; THE DIMENSIONLESS AMPLITUDE FUNCTION,
C       'RAMP'; AND THE DIMENSIONLESS INTENSITY FUNCTION, 'RINT' (MULTIPLIED BY
C       THE SIZE OF THE INTERVAL FOR CONVENIENCE).  THE COMPUTATION IS FOR VALUES
C       OF X AS SPECIFIED BY THE USER IN LINES 18 AND23 FOR SPECIFIED VALUE OF
C       WAVELENGTH (LINE15) AND COMPLEX INDEX OF REFRACTION (LINE 2).
C       THE SECOND PORTION OF THIS PROGRAM - LINE63 THRU 118 - COMPUTES THE
C       EXTINCTION, SCATTERING, AND BACKSCATTER COEFFICIENTS, LABELED 'BEXT#',
C       'BSC#',  AND 'BPI#'' RESPECTIVELY, IN UNITS OF INVERSE METERS FOR THE
C       FIRST TWO, AND INVERSE (METERS-STERADIANS) FOR THE LAST COEFFICIENT.  THE
C       INTEGRATION OF THESE FUNCTIONS IS BY TRAPEZOIDAL RULE AND INCLUDES SUCH
C       DISTRIBUTION FUNCTIONS (FUN#) AS SPECIFIED BY THE USER.
C       THE THIRD PORTION - LINE118 THRU 155 - COMPUTES THE RATIO OF TRANSMITTED
C       INTENSITY TO RECEIVED INTENSITY, BUT DOES NOT INCLUDE THE TRANSMISSIVITY
C       OF THE INTERVENING MEDIUM.  HOWEVER, THE LATTER MAY BE INCLUDED AS A MULTI
C       PLICATIVE CONSTANT IN LINE 147.
C       PRINT OUT INCLUDES PRINTING THE EXTINCTION AND SCATTERING EFFICIENCIES AND
C       THE AMPLITUDE FUNCTION VERSUS X FOR SELECTED VALUES OF X (DETERMINED BY
C       LINES 110,111).  IT ALSO INCLUDES PRINTING THE BEXT,BSC,BPI, FOR EACH OF
C       FOUR DISTRIBUTION FUNCTIONS AND THE RATIO OF INTENSITIES (BACKSCATTER) FOR
C       A FIELD OF VIEW - SCATTERING AREA FUNCTION (SOLID ANGLE) AND VARIOUS
C       VALUES OF SCATTERING VOLUME LENGTH (RESOLUTION) AS DETERMINED BY LINE 144.
C       NOTE 2:  TO ADJUST THIS PROGRAM TO A SPECIFIC NEED, ONE MUST ALTER THE
C       LINE(S) IN PARENTHESIS FOLLOWING THE SPECIFIED FUNCTION:  WAVELENGTH (15,
C       146), COMPLEX INDEX OF REFRACTION (2,26,27), LIMITS OF X (18,23,81,82,83,
C       110,111), VARIATION OF X (18,60,79,80,110), FIELD OF VIEW AND/OR SCATTER-
C       ING AREA (146), LENGTH OF SCATTERING VOLUME (144).  FOR FURTHER OPTIONS,
C       SEE TEXT.
```

```
      COMPLEX A(300),B(300),D(300),W(300),AMP,ANBN,CMPLX,RM,RMX,RAMP
      RM=CMPLX(1.212,-0.0601)
      BEXT1=0.0
      BEXT2=0.0
      BEXT3=0.0
      BEXT4=0.0
      BSC1=0.0
      BSC2=0.0
      BSC3=0.0
      BSC4=0.0
      BPI1=0.0
      BPI2=0.0
      BPI3=0.0
      BPI4=0.0
      U=10.6
      WRITE(6,10)
   10 FORMAT(/3X,'X',13X,'KEXT',10X,'KSC',21X,'S1'/)
      DO 200 MM=1,1471,15
      SKEXT=0.0
      SKSC=0.0
      RAMP=CMPLX(0.0,0.0)
      AMP=CMPLX(0.0,0.0)
      XN=MM*0.01
      SXN=SIN(XN)
      CXN=COS(XN)
      P=XN*1.212
      Q=XN*(-0.0601)
      RMX=CMPLX(P,Q)
      M=1.2*XN+12
      W(1)=CMPLX(CXN,-SXN)
```

```
      W(2)=CMPLX(SXN,CXN)
      SINP=SIN(P)
      COSP=COS(P)
      SINHQ=(EXP(Q)-EXP(-Q))/2
      COSHQ=(EXP(Q)+EXP(-Q))/2
      DIV=((SINP**2)*(COSHQ**2))+((COSP**2)*(SINHQ**2))
      RMR=COSP*SINP/DIV
      RMI=-(SINHQ*COSHQ/DIV)
      D(2)=CMPLX(RMR,RMI)
      DO 150 N=3,M,1
      W(N)=(((2*(N-2))-1)*W(N-1)/XN)-W(N-2)
      D(N)=(-(N-2)/RMX)+(1/(((N-2)/RMX)-D(N-1)))
      RWN=REAL(W(N))
      RWN1=REAL(W(N-1))
      A(N)=(RWN*(((N-2)/XN)+(D(N)/RM))-RWN1)/
     *(W(N)*(((N-2)/XN)+(D(N)/RM))-W(N-1))
      B(N)=(RWN*(((N-2)/XN)+(D(N)*RM))-RWN1)/
     *(W(N)*(((N-2)/XN)+(D(N)*RM))-W(N-1))
      PI=-((-1)**(N-2))*((N-2)*(N-1))/2
      AMP=((2.*(N-2))+1)*PI*(A(N)-B(N))/((N-2)*(N-1))
      RAMP=RAMP+AMP
      ANBN=A(N)+B(N)
      RANBN=REAL(ANBN)
      SKEXTN=(2*(N-2)+1)*RANBN
      SKEXT=SKEXT+SKEXTN
      R=CABS(A(N))
      S=CABS(B(N))
      SKSCN=(2*(N-2)+1)*(R**2+S**2)
      SKSC=SKSC+SKSCN
  150 CONTINUE
      RAMPN=CABS(RAMP)
      RINT=0.15*(RAMPN**2.0)
      EXT=2.0*SKEXT/(XN**2.0)
      SCT=2.0*SKSC/(XN**2.0)
      R=XN*U/(2.0*3.1415926)
      XDK1=R**1.33333
      XDK23=R**2.0
      XDK4=R**3.0
      XDK5=R**5.0
      XDK6=R**6.0
      XDK8=R**8.0
      AA=0.11098E-06
      BB=0.7901E-03
      FUN1=23.480232*XDK4*EXP(-0.42341*XDK1)
      FUN2=1.0*XDK5*EXP(-0.1*XDK23)
      FUN3=0.0078248*XDK5*EXP(-0.025*XDK23)
      FUN4=AA*XDK8*EXP(-BB*XDK4)
      H1=((U/(2.0*3.1415926))**3.0)*(1.00E-06)
      H2=H1
      H4=H1
```

```
      CON1=2.0*3.1415926*0.15*SKEXT
      CON2=2.0*3.1415926*0.15*SKSC
      FIRST=XN-0.01
      LAST1=XN-9.61
      LAST2=XN-14.71
      IF (FIRST) 200,160,155
  155 IF(LAST1)180,165,158
  158 IF(LAST2)182,170,200
  160 FUN1=FUN1/2.0
      FUN2=FUN2/2.0
      FUN3=FUN3/2.0
      FUN4=FUN4/2.0
      GO TO 180
  165 FUN1=FUN1/2.0
      GO TO 180
  170 FUN2=FUN2/2.0
      FUN3=FUN3/2.0
      FUN4=FUN4/2.0
      GO TO 182
  180 BEXT1=BEXT1+(CON1*FUN1*H1)
      BSC1=BSC1+(CON2*FUN1*H1)
      BPI1=BPI1+(RINT*FUN1*H4)
  182 BEXT2=BEXT2+(CON1*FUN2*H2)
      BSC2=BSC2+(CON2*FUN2*H2)
      BPI2=BPI2+(RINT*FUN2*H4)
      BEXT3=BEXT3+(CON1*FUN3*H2)
      BSC3=BSC3+(CON2*FUN3*H2)
      BPI3=BPI3+(RINT*FUN3*H4)
      BEXT4=BEXT4+(CON1*FUN4*H2)
      BSC4=BSC4+(CON2*FUN4*H2)
      BPI4=BPI4+(RINT*FUN4*H4)
      DO 195 N=151,1501,150
      YN=N*0.01
      DIFF=XN-YN
      IF(DIFF)200,185,195
  185 WRITE(6,190)XN,EXT,SCT,RAMP
  190 FORMAT(5E14.6//)
      GO TO 200
  195 CONTINUE
  200 CONTINUE
      DO 300 J=1,4,1
      WRITE(6,205)
  205 FORMAT(4X,'J',5X,'BEXT',10X,'BSC',11X,'B(PI)'/)
      GO TO (210,220,230,240),J
  210 WRITE(6,215)J,BEXT1,BSC1,BPI1
  215 FORMAT(2X,I3,2X,3E14.6/)
      BEXT=BEXT1
      BETA=BPI1
      GO TO 280
```

```
      220 WRITE(6,225)J,BEXT2,BSC2,BPI2
      225 FORMAT(2X,I3,2X,3E14.6/)
          BEXT=BEXT2
          BETA=BPI2
          GO TO 280
      230 WRITE(6,235)J,BEXT3,BSC3,BPI3
      235 FORMAT(2X,I3,2X,3E14.6/)
          BEXT=BEXT3
          BETA=BPI3
          GO TO 280
      240 WRITE(6,245)J,BEXT4,BSC4,BPI4
      245 FORMAT(2X,I3,2X,3E14.6/)
          BEXT=BEXT4
          BETA=BPI4
      280 WRITE(6,282)
      282 FORMAT(/3X,'RESOLUTION',4X,'SOLID ANGLE',3X,'BACKSCATTER'/
          DO 290 L=1,10,1
          RESO=L
          OMEGA=0.616E-08
          BACKSC=RESO*OMEGA*BETA*EXP(-2*RESO*BEXT)
          WRITE (6,285)RESO,OMEGA,BACKSC
      285 FORMAT(/3E14.6/)
          DELTA=BACKSC-1.00E-50
          IF(DELTA)300,300,290
      290 CONTINUE
      300 CONTINUE
          STOP
          END

     $EXEC
```

X	KEXT	KSC	S1	
0.151000E 01	0.381408E 00	0.129208E 00	0.826519E-01	0.116796E 00
0.301000E 01	0.108916E 01	0.597752E 00	-0.185405E 00	0.159753E-01
0.451000E 01	0.181213E 01	0.114461E 01	-0.104220E 00	0.449025E-01
0.601000E 01	0.237685E 01	0.157640E 01	-0.141711E 00	-0.438158E 00
0.751000E 01	0.270829E 01	0.181043E 01	0.384792E 00	0.168074E 00
0.901000E 01	0.281911E 01	0.184958E 01	-0.253443E 00	-0.307156E 00

```
0.105100E 02  0.276733E 01  0.174417E 01  0.684621E 00  0.273401E 00

0.120100E 02  0.262605E 01  0.156476E 01 -0.523891E 00  0.519301E-01

0.135100E 02  0.246690E 01  0.137922E 01  0.604395E 00  0.212389E 00

  J      BEXT           BSC            B(PI)

  1    0.391808E-01  0.229474E-01  0.640959E-04

 RESOLUTION     SOLID ANGLE    BACKSCATTER

0.100000E 01  0.616000E-08  0.365072E-12

0.200000E 01  0.616000E-08  0.675113E-12

0.300000E 01  0.616000E-08  0.936345E-12

0.400000E 01  0.616000E-08  0.115436E-11

0.500000E 01  0.616000E-08  0.133420E-11

0.600000E 01  0.616000E-08  0.148037E-11

0.700000E 01  0.616000E-08  0.159692E-11

0.800000E 01  0.616000E-08  0.168750E-11

0.900000E 01  0.616000E-08  0.175535E-11

0.100000E 02  0.616000E-08  0.180339E-11

  J      BEXT           BSC            B(PI)

  2    0.130680E 00  0.777407E-01  0.199547E-03
```

RESOLUTION	SOLID ANGLE	BACKSCATTER
0.100000E 01	0.616000E-08	0.946496E-12
0.200000E 01	0.616000E-08	0.145761E-11
0.300000E 01	0.616000E-08	0.168355E-11
0.400000E 01	0.616000E-08	0.172845E-11
0.500000E 01	0.616000E-08	0.166364E-11
0.600000E 01	0.616000E-08	0.153721E-11
0.700000E 01	0.616000E-08	0.138093E-11
0.800000E 01	0.616000E-08	0.121523E-11
0.900000E 01	0.616000E-08	0.105269E-11
0.100000E 02	0.616000E-08	0.900642E-12

J	BEXT	BSC	B(PI)
3	0.473336E 00	0.310621E 00	0.210000E-03

RESOLUTION	SOLID ANGLE	BACKSCATTER
0.100000E 01	0.616000E-08	0.501957E-12
0.200000E 01	0.616000E-08	0.389550E-12
0.300000E 01	0.616000E-08	0.226736E-12

0.400000E 01 0.616000E-08 0.117307E-12

0.500000E 01 0.616000E-08 0.568984E-13

0.600000E 01 0.616000E-08 0.264940E-13

0.700000E 01 0.616000E-08 0.119939E-13

0.800000E 01 0.616000E-08 0.531885E-14

0.900000E 01 0.616000E-08 0.232186E-14

0.100000E 02 0.616000E-08 0.100106E-14

J	BEXT	BSC	B(PI)
4	0.300532E 00	0.192589E 00	0.100082E-03

RESOLUTION	SOLID ANGLE	BACKSCATTER
0.100000E 01	0.616000E-08	0.337985E-12
0.200000E 01	0.616000E-08	0.370585E-12
0.300000E 01	0.616000E-08	0.304748E-12
0.400000E 01	0.616000E-08	0.222762E-12
0.500000E 01	0.616000E-08	0.152655E-12
0.600000E 01	0.616000E-08	0.100428E-12
0.700000E 01	0.616000E-08	0.642335E-13
0.800000E 01	0.616000E-08	0.402453E-13
0.900000E 01	0.616000E-08	0.248215E-13
0.100000E 02	0.616000E-08	0.151198E-13

APPENDIX D

DATA

The tables that follow are the output of the computer program. The Mie parameters are not included here since their tabulation is not directly related to the major emphasis of this study. An example has been included in the actual computer printout contained in Appendix C.

For all tables, an explanation of terms is given as follows: Exponents are expressed as follows: $1.5\times10^{-2} = 1.5 - 0.2$

Resolution ≡ length of scattering volume

Solid Angle ≡ scattering area × field of view

Backscatter ≡ $\frac{I_{RECEIVER}}{H(\lambda)}$. It does not include transmissivity of intervening medium.

Table D1. Intensity Ratios for Distribution 1; Wavelength = 10.6 μm, Δx = 0.15; β_{ext} = 3.91808-02m^{-1}; β_{sc} = 2.29474-02m^{-1}; $\beta(\pi)$ = 6.40959-05 m^{-1}-sr^{-1}.

Resolution (Meters)	Solid Angle (Meter)^2(Steradian)	BACKSCATTER (Dimensionless)
1.0	6.16-09	3.65072-13
2.0	"	6.76113-13
3.0	"	9.36345-13
4.0	"	1.15436-12
5.0	"	1.33420-12
6.0	"	1.48037-12
7.0	"	1.59692-12
8.0	"	1.68750-12
9.0	"	1.75535-12
10.0	"	1.80339-12

Table D2. Intensity Ratios for Distribution 2; Wavelength = 10.6 μm, Δx = 0.15; β_{ext} = 1.30680-01 m^{-1}; β_{sc} = 7.77407-02 m^{-1}; $\beta(\pi)$ = 1.99547-04 m^{-1}-sr^{-1}.

Resolution (Meters)	Solid Angle (Meter)^2(Steradian)	BACKSCATTER (Dimensionless)
1.0	6.16-09	9.46496-13
2.0	"	1.45761-12
3.0	"	1.68355-12
4.0	"	1.72845-12
5.0	"	1.66364-12
6.0	"	1.53721-12
7.0	"	1.38093-12
8.0	"	1.21523-12
9.0	"	1.05269-12
10.0	"	9.00642-13

Table D3. Intensity Ratios for Distribution 3; Wavelength = 10.6 μm, $\Delta x = 0.15$; $\beta_{ext} = 4.73336\text{-}01\ m^{-1}$; $\beta_{sc} = 3.10621\text{-}01\ m^{-1}$; $\beta(\pi) = 2.10000\text{-}04\ m^{-1}\text{-}sr^{-1}$.

Resolution (Meters)	Solid Angle $(Meter)^2(Steradian)$	BACKSCATTER (Dimensionless)
1.0	6.16-09	5.01957-13
2.0	"	3.89550-13
3.0	"	2.26736-13
4.0	"	1.17307-13
5.0	"	5.68984-14
6.0	"	2.64940-14
7.0	"	1.19939-14
8.0	"	5.31885-15
9.0	"	2.32186-15
10.0	"	1.00106-15

Table D4. Intensity Ratios for Distribution 4; Wavelength = 10.6 μm, Δx = 0.15; β_{ext} = 3.00532-01 m^{-1}; β_{sc} = 1.92589-01 m^{-1}; $\beta(\pi)$ = 1.00082-04 m^{-1}-sr^{-1}

Resolution (Meters)	Solid Angle $(Meter)^2$(Steradian)	BACKSCATTER (Dimensionless)
1.0	6.16-09	3.37895-13
2.0	"	3.70585-13
3.0	"	3.04748-13
4.0	"	2.22762-13
5.0	"	1.52655-13
6.0	"	1.00428-13
7.0	"	6.42335-14
8.0	"	4.02453-14
9.0	"	2.48215-14
10.0	"	1.51198-14

Table D5. Intensity Ratios for Distribution 1; Wavelength = 4.0 μm, $\Delta x = 0.40$; $\beta_{ext} = 8.46463\text{-}02\ m^{-1}$; $\beta_{sc} = 7.78943\text{-}02\ m^{-1}$; $\beta(\pi) = 1.24974\text{-}03\ m^{-1}\text{-}sr^{-1}$

Resolution (Meters)	Solid Angle $(Meter)^2(Steradian)$	BACKSCATTER (Dimensionless)
1.0	8.77-10	9.25329-13
2.0	"	1.56244-12
3.0	"	1.97866-12
4.0	"	2.22735-12
5.0	"	2.35058-12
6.0	"	2.38141-12
7.0	"	2.34562-12
8.0	"	2.26322-12
9.0	"	2.14959-12
10.0	"	2.01647-12

AD-A052 636 OKLAHOMA UNIV NORMAN DEPT OF ENGINEERING PHYSICS F/G 4/2
A STUDY OF THE APPLICABILITY OF LASERS TO THE MEASUREMENT OF TO--ETC(U)
1976 D A ROSS

UNCLASSIFIED NL

2 OF 2
AD
AD52636

END
DATE
FILMED
5-78
DDC

Table D6. Intensity Ratios for Distribution 2; Wavelength = 4.0 μm, $\Delta x = 0.40$; $\beta_{ext} = 2.40473\text{-}01\ m^{-1}$; $\beta_{sc} = 2.18361\text{-}01\ m^{-1}$; $\beta(\pi) = 3.87723\text{-}03\ m^{-1}\text{-}sr^{-1}$

Resolution (Meters)	Solid Angle (Meter)^2(Steradian)	BACKSCATTER (Dimensionless)
1.0	8.77-10	2.10208-12
2.0	"	2.59900-12
3.0	"	2.41005-12
4.0	"	1.98652-12
5.0	"	1.53508-12
6.0	"	1.13878-12
7.0	"	8.21324-13
8.0	"	5.80276-13
9.0	"	4.03567-13
10.0	"	2.77205-13

Table D7. Intensity Ratios for Distribution 3; Wavelength = 4.0 μm, Δx = 0.40; β_{ext} = 4.32330-01 m^{-1}; β_{sc} = 3.59059-01 m^{-1}; $\beta(\pi)$ = 1.18300-02 m^{-1}-sr^{-1}

Resolution (Meters)	Solid Angle (Meter)^2(Steradian)	BACKSCATTER (Dimensionless)
1.0	8.77-10	4.36984-12
2.0	"	3.68111-12
3.0	"	2.32569-12
4.0	"	1.30609-12
5.0	"	6.87648-13
6.0	"	3.47560-13
7.0	"	1.70789-13
8.0	"	8.22118-14
9.0	"	3.89556-14
10.0	"	1.82310-14

Table D8. Intensity Ratios for Distribution 4; Wavelength = 4.0 μm, Δx = 0.40; β_{ext} = 2.46862-01 m^{-1}; β_{sc} = 1.96040-01 m^{-1}; $\beta(\pi)$ = 3.37952-03 m^{-1}-sr^{-1}

Resolution (Meters)	Solid Angle (Meter)^2(Steradian)	BACKSCATTER (Dimensionless)
1.0	8.77-10	1.80897-12
2.0	"	2.20821-12
3.0	"	2.02167-12
4.0	"	1.64523-12
5.0	"	1.25520-12
6.0	"	9.19334-13
7.0	"	6.54633-13
8.0	"	4.56634-13
9.0	"	3.13544-13
10.0	"	2.12635-13

Table D9. *Intensity Ratios for Distribution 1; Wavelength* = 1.06 μm, Δx = 1.5; β_{ext} = 6.80013-02 m^{-1}; β_{sc} = 6.80013-02 m^{-1}; $\beta(\pi)$ = 3.59016-03 m^{-1}-sr^{-1}

Resolution (Meters)	Solid Angle (Meter)^2(Steradian)	BACKSCATTER (Dimensionless)
1.0	6.16-11	1.93032-13
2.0	"	3.36972-13
3.0	"	4.41184-13
4.0	"	5.13444-13
5.0	"	5.60193-13
6.0	"	5.86751-13
7.0	"	5.97497-13
8.0	"	5.96023-13
9.0	"	5.85261-13
10.0	"	5.67600-13

Table D10. Intensity Ratios for Distribution 2; Wavelength = 1.06 μm, $\Delta x = 1.5$; $\beta_{ext} = 2.06574\text{-}01\ m^{-1}$; $\beta_{sc} = 2.06574\text{-}01\ m^{-1}$; $\beta(\pi) = 1.05844\text{-}02\ m^{-1}\text{-}sr^{-1}$

Resolution (Meters)	Solid Angle $(Meter)^2(Steradian)$	BACKSCATTER (Dimensionless)
1.0	6.16-11	4.31341-13
2.0	"	5.70719-13
3.0	"	5.66351-13
4.0	"	4.99570-13
5.0	"	4.13122-13
6.0	"	3.27968-13
7.0	"	2.53134-13
8.0	"	1.91388-13
9.0	"	1.42443-13
10.0	"	1.04705-13

Table D11. Intensity Ratios for Distribution 3; Wavelength = 1.06 μm, $\Delta x = 1.5$; $\beta_{ext} = 3.99796\text{-}01\ m^{-1}$; $\beta_{sc} = 3.99796\text{-}01\ m^{-1}$; $\beta(\pi) = 2.31075\text{-}02\ m^{-1}\text{-}sr^{-1}$

Resolution (Meters)	Solid Angle $(Meter)^2(Steradian)$	BACKSCATTER (Dimensionless)
1.0	6.16-11	6.39845-13
2.0	"	5.75237-13
3.0	"	3.87864-13
4.0	"	2.32466-13
5.0	"	1.30621-13
6.0	"	7.04586-14
7.0	"	3.69507-14
8.0	"	1.89826-14
9.0	"	9.59955-15
10.0	"	4.79457-15

Table D12. Intensity Ratios for Distribution 4; Wavelength = 1.06 μm, $\Delta x = 1.5$; $\beta_{ext} = 2.31788\text{-}01\ m^{-1}$; $\beta_{sc} = 2.31788\text{-}01\ m^{-1}$; $\beta(\pi) = 1.21906\text{-}02\ m^{-1}\text{-}sr^{-1}$

Resolution (Meters)	Solid Angle $(Meter)^2(Steradian)$	BACKSCATTER (Dimensionless)
1.0	6.16-11	4.72363-13
2.0	"	5.94261-13
3.0	"	5.60713-13
4.0	"	4.70274-13
5.0	"	3.69771-13
6.0	"	2.79117-13
7.0	"	2.04835-13
8.0	"	1.47254-13
9.0	"	1.04206-13
10.0	"	7.28318-14

Table D13. Intensity Ratios for Distribution 1; Wavelength = 0.5 μm, Δx = 3.15; β_{ext} = 6.53955-02 m^{-1}; β_{sc} = 6.53955-02 m^{-1}; $\beta(\pi)$ = 3.49286-03 m^{-1}-sr^{-1}

Resolution (Meters)	Solid Angle $(Meter)^2$(Steradian)	BACKSCATTER (Dimensionless)
1.0	1.37-11	4.19855-14
2.0	"	7.36763-14
3.0	"	9.69655-14
4.0	"	1.13437-13
5.0	"	1.24412-13
6.0	"	1.30991-13
7.0	"	1.34087-13
8.0	"	1.34455-13
9.0	"	1.32717-13
10.0	"	1.29385-13

Table D14. Intensity Ratios for Distribution 2; Wavelength = 0.5 μm, $\Delta x = 3.15$; $\beta_{ext} = 1.99431\text{-}01\ m^{-1}$; $\beta_{sc} = 1.99431\text{-}01\ m^{-1}$; $\beta(\pi) = 8.69341\text{-}03\ m^{-1}\text{-}sr^{-1}$

Resolution (Meters)	Solid Angle (Meter)^2(Steradian)	BACKSCATTER (Dimensionless)
1.0	1.37-11	7.99258-14
2.0	"	1.07274-13
3.0	"	1.07984-13
4.0	"	9.66220-14
5.0	"	8.10518-14
6.0	"	6.52710-14
7.0	"	5.11027-14
8.0	"	3.91933-14
9.0	"	2.95897-14
10.0	"	2.20635-14

Table D15. Intensity Ratios for Distribution 3; Wavelength = 0.5 μm, Δx = 3.15; β_{ext} = 3.90475-01 m^{-1}; β_{sc} = 3.90475-01 m^{-1}; $\beta(\pi)$ = 2.49455-02 m^{-1}-sr^{-1}

Resolution (Meters)	Solid Angle (Meter)^2(Steradian)	BACKSCATTER (Dimensionless)
1.0	1.37-11	1.56513-13
2.0	"	1.43357-13
3.0	"	9.84801-14
4.0	"	6.01347-14
5.0	"	3.44250-14
6.0	"	1.89187-14
7.0	"	1.01083-14
8.0	"	5.29063-15
9.0	"	2.72582-15
10.0	"	1.38705-15

Table D16. Intensity Ratios for Distribution 4; Wavelength = 0.5 μm, $\Delta x = 3.15$; $\beta_{ext} = 2.27353\text{-}01\ m^{-1}$; $\beta_{sc} = 2.27353\text{-}01\ m^{-1}$; $\beta(\pi) = 1.44447\text{-}02\ m^{-1}\text{-}sr^{-1}$

Resolution (Meters)	Solid Angle $(Meter)^2(Steradian)$	BACKSCATTER (Dimensionless)
1.0	1.37-11	1.25589-13
2.0	"	1.59407-13
3.0	"	1.51747-13
4.0	"	1.28405-13
5.0	"	1.01863-13
6.0	"	7.75750-14
7.0	"	5.74371-14
8.0	"	4.16590-14
9.0	"	2.97430-14
10.0	"	2.09733-14

BIBLIOGRAPHY

Abbey, Robert F., Jr. *9th Conference on Severe Local Storms* (Norman, Oklahoma, 1975).

Anderson, R. C., and E. V. Browell. "First- and Second-Order Backscattering from Clouds Illuminated by Finite Beam." *Applied Optics 11:6* (June, 1972).

Carrier, L. W., G. A. Cato, and K. J. von Essen. "The Backscattering and Extinction of Visible and Infrared Radiation by Selected Major Cloud Models," *Applied Optics 6:7* (July, 1967).

Charschan, S. S. ed., *Lasers in Industry*. New York: van Nostrand Reinhold Company, 1972.

Dave, J. V. "Subroutines for Computing the Parameters of the Electromagnetic Radiation Scattered by a Sphere." Report prepared for IBM, Rep. 320-3237. Palo Alto, CA: IBM Scientific Center, 1968.

Dave J. V. "Effect of Coarseness of the Integration Increment on the Calculation of the Radiation Scattered by Polydispersed Aerosols." *Applied Optics 8:6* (June, 1969).

Dave, J. V. "Effect of Varying Integration Increment on the Computed Polarization Characteristics of the Radiation Scattered by Polydispersed Aerosols." *Applied Optics 8:10* (October, 1969).

Davies-Jones, Robert and Edwin Kessler. "Tornadoes," *Weather and Climate Modification*, ed. Wilmot N. Hess (New York: John Wiley and Sons, Inc., 1974).

Deirmendjian, D. and R. J. Clasen. *Light Scattering on Partially Absorbing Homogeneous Spheres of Finite Size*. Report prepared for United States Air Force Project Rand, #R-393-PR, February, 1962. Santa Monica, CA: Rand Corporation, 1962.

Deirmendjian, D. *Scattering and Polarization Properties of Polydispersed Suspensions with Partial Absorption*. Report prepared for United States Air Force Project Rand, Memo #RM-3228-PR, July, 1962. Santa Monica, CA: Rand Corporation, 1962.

Deirmendjian, D. *Tables of Mie Scattering Cross Sections and Amplitudes*. Report prepared for United States Air Force Project Rand, #R-407-PR, January, 1963. Santa Monica, CA: Rand Corporation, 1963.

Deirmendjian, D. *Electromagnetic Scattering on Spherical Polydispersions* (New York: American Elsevier Publishing Company, Inc., 1969).

Elterman, Louis and Robert B. Toolin. "Atmospheric Optics." *Handbook of Geophysics and Space Environments.* Edited by Shea L. Valley. New York: McGraw-Hill Co., 1965.

French, A. P. *Special Relaivity.* New York: W. W. Norton and Co. Inc., 1968.

Gumprecht, R. O. and C. M. Sliepcevich. *Light-Scattering Functions for Spherical Particles.* Willow Run Research Center: University of Michigan Press, 1951.

Houghton, H. G. and W. R. Chalker. "The Scattering Cross Section of Water Drops in Air for Visible Light," *Journal of the Optical Society of America 39:11* (November, 1949).

Howard, John N.; John S. Garing, and Russell G. Walker. "Transmission and Detection of Infrared Radiation." *Handbook of Geophysics and Space Environments.* Edited by Shea L. Valley. New York: McGraw-Hill Co., 1965.

Hulst, H. C. van de. *Light Scattering by Small Particles.* New York: John Wiley and Sons, Inc., 1957.

Kreysize, E. *Advanced Engineering Mathematics. 3d ed.* New York: John Wiley and Sons, Inc., 1972.

Kruse, Paul W.; Laurence D. McGlauchlin, and Richard B. McQuistan. *Elements of Infrared Technology.* New York: John Wiley and Sons, Inc., 1962.

Longhurst, R. S. *Geometrical and Physical Optics. 3d ed.* London: Longman Group Limited, 1973.

McCarthy, John. Personal Interview, Meteorology Dept., OU, September, 1975.

McCoy, John H.; David B. Rensch, and Ronald K. Long. "Water Vapor Continuum Absorption of Carbon Dioxide Laser Radiation Near 10μ." *Applied Optics 8:7* (July, 1969).

Pratt, William K. *Laser Communication Systems.* New York: John Wiley and Sons, Inc., 1969.

Rensch, D. B. and R. K. Long, "Comparative Studies of Extinction and Backscattering by Aerosols, Fog, and Rain at 10.6μ and 0.63 μ," *Applied Optics 9:7* (July, 1970).

Siegman, A. E. *An Introduction to Lasers and Masers.* New York: McGraw-Hill Co., 1971.

Simpson, Joanne and Victor Wiggert. "Models of Precipitating Cumulus Towers." *Monthly Weather Review 97:7* (July, 1969).

Weast, Robert C., ed. *Handbook of Chemistry and Physics*. 54th ed. Cleveland: CRC Press, 1973.

Woodman, Douglas P. "Limitations in Using Atmospheric Models for Laser Transmission Estimates." *Applied Optics 13:10* (October, 1974).

Wyatt, Philip J.; Robert V. Stull, and Gilbert N. Plass. "The Infrared Transmittance of Water Vapor." *Applied Optics 3:2* (February, 1964).

Wyatt, Philip J.: Robert V. Stull, and Gilbert N. Plass. "The Infrared Transmittance of Carbon Dioxide." *Applied Optics 3:2* (February, 1964).

Yin, P.K.L. and R. K. Long. "Atmospheric Absorption at the Line Center of P(20) CO_2 Laser Radiation." *Applied Optics 7:8* (August, 1968).